Study, design, and characterization of anchor loss reduction and tuning the frequency of MEMS resonators for timing applications

by

Mohammad KAZEMI

THESIS PRESENTED TO ÉCOLE DE TECHNOLOGIE SUPÉRIEURE
IN PARTIAL FULFILLMENT OF A MASTER'S DEGREE
WITH THESIS IN ELECTRICAL ENGINEERING
M.A.Sc.

MONTREAL, AUGUST 25, 2023

ÉCOLE DE TECHNOLOGIE SUPÉRIEURE
UNIVERSITÉ DU QUÉBEC

BOARD OF EXAMINERS

THIS THESIS HAS BEEN EVALUATED

BY THE FOLLOWING BOARD OF EXAMINERS

M. Frédéric Nabki, memorandum supervisor
Department of Electrical Engineering, École de technologie supérieure

M. Michael Ménard, president of the board of examiners
Department of Electrical Engineering, École de technologie supérieure

M. Ricardo Izquierdo, member of the jury
Department of Electrical Engineering, École de technologie supérieure

THIS THESIS WAS PRESENTED AND DEFENDED

IN THE PRESENCE OF A BOARD OF EXAMINERS AND THE PUBLIC

ON "7, JULY, 2023"

AT ÉCOLE DE TECHNOLOGIE SUPÉRIEURE

ACKNOWLEDGEMENTS

First and foremost, I would like to express my sincere gratitude to my thesis supervisor, Professor Frederic Nabki. I am particularly grateful for his trust in me, the independence he provided, and his wise guidance throughout my research, which has made this thesis what it is today. He has granted me an invaluable opportunity to gain knowledge and experience in the field I was eager to study. Thank you for your unwavering support and guidance, Frederic.

I would also like to thank the co-authors of my articles, in particular Mathieu Gratuze and Seyed Fakhredin (Koorosh) Nabavi, and also my colleagues and friends in the Laboratory of Communications and Integration of the MicroÉlectronique (LaCIME) and my other friends at the École de Technologie Supérieure (Amin, Amirreza, Nakisa, Narges, Julian,...).

I would also like to thank CMC Microsystems, which provided the design tools and allowed the manufacture of the various MEMS chips that I designed for my research.

Finally, I would like to express my heartfelt gratitude to my beloved mother, father, and sisters for their unwavering support throughout my life and academic pursuits. Their encouragement and guidance have been instrumental in my success. In addition, I want to extend my sincere appreciation to two of my closest friends, Hamid Ghasemi and Moein Moradi, and Kambiz Kalhor. They have been a constant source of support and encouragement, always there to lend an ear and offer guidance when I needed it most.

Étude, conception et caractérisation de la réduction de la perte d'ancrage et de l'accord de fréquence des résonateurs MEMS en forme de poutre pour les applications de synchronisation

Mohammad KAZEMI

RÉSUMÉ

Les appareils électriques et toutes les machines qui comportent une partie électronique ont besoin d'une synchronisation précise pour être fonctionnels. La nécessité d'une synchronisation précise s'accroît avec la croissance considérable des télécommunications à haut débit et du traitement des données. Le besoin de dispositifs compacts et de circuits électroniques qui peuvent fonctionner encore mieux et plus rapidement nécessite de nouvelles générations de microsystèmes électromécaniques (MEMS).

L'objectif de ce travail est de contribuer au développement des connaissances accumulées en matière de perte d'ancrage et d'accordabilité des dispositifs résonants MEMS.

Une revue de littérature approfondie a été effectuée au début de ce travail pour présenter les dispositifs MEMS, leurs applications et leurs procédés de fabrication. Ensuite, la modélisation, la conception et la fabrication de dispositifs résonants MEMS en forme de poutre sont présentées en mettant l'accent sur la réduction des pertes d'ancrage. L'avantage de ce travail est d'illustrer l'effet de différentes formes de trous réflecteurs d'énergie qui sont placés sur la structure d'ancrage, sur la perte d'ancrage et sur le facteur de qualité poutres résonantes.

L'étude d'un résonateur MEMS dont la fréquence d'opération est accordable est ensuite présentée. Dans ce travail, deux actionneurs DC avec des ressorts sont utilisés pour changer la fréquence des poutres résonnantes en touchant les ancres, ce qui conduit à l'augmentation de la rigidité du ressort des ancres et donc à l'augmentation de la fréquence du résonateur. L'avantage de ce travail est la structure simple qui apporte une haute accordabilité de la structure résonante.

Mots-clés: Résonateurs MEMS, facteur de qualité, perte d'ancrage, PiezoMUMPs, réglage de la fréquence de résonance, actionneurs DC

Study, design, and characterization of anchor loss reduction and tuning the frequency of MEMS resonators for timing applications

Mohammad KAZEMI

ABSTRACT

Electrically powered devices and machines with electronic components require precise timing to function properly. The need for accuracy has become increasingly critical with the growth of high-speed telecommunications and data processing. To meet the demand for more efficient and faster electronic circuits and compact devices, the development of new generations of micro-electromechanical systems (MEMS) is necessary.

The purpose of this study is to contribute to the advancement of knowledge on anchor loss and tunability of MEMS resonant devices.

To begin, a comprehensive review of the literature was conducted to provide an overview of MEMS devices, their applications, and fabrication processes. Next, this thesis presents the modeling, design, and fabrication of clamped-clamped beam MEMS resonant devices with a focus on reducing anchor loss. The work examines the impact of different shapes of energy reflector holes on the anchoring structure's anchor loss and the beam resonator's quality factor.

This thesis also explores the design and fabrication of a tunable MEMS resonator. The device comprises a resonator anchored on both sides through suspended beams, situated between two DC actuators with springs. The activation of each actuator increases the frequency of the resonator through the added stiffness of the anchoring structure and resonator. The simplicity of the structure provides high tunability of the resonant structure, which is a notable advantage of this work.

Keywords: MEMS resonators, Quality factor, Anchor loss, PiezoMUMPs, Resonance frequency tuning, DC actuators

TABLE OF CONTENTS

Page

LIST OF TABLES

LIST OF FIGURES

LIST OF ABREVIATIONS

Al	Aluminium
AlN	Nitrure d'aluminium
Cr	Chrome
ETS	École de Technologie Supérieure
FBAR	Thin-Film Bulk Acoustic Resonator
FEM	Finite Element Modelling
GSG	Ground-Signal-Ground
IC	Integrated Circuit
IoT	Internet of Things
IEEE	Institute of Electrical and Electronics Engineers
LaCIME	(french, Laboratoire de Communications et d'Intégration de la MicroÉlectronique)
MEMS	Microelectromechanical System
PML	Perfectly Matched Layer
SEM	Scanning Electron Microscope
Q	Quality Factor
PZT	Titano-Zirconate
SAW	Surface Acoustic Wave Resonator
SOI	Silicon On Insulator
VNA	Vectorial Network Analyzer

GND	Ground
TUB	Thin-film Under Bulk

LIST OF SYMBOLS AND UNITS OF MEASUREMENTS

ρ	Density
E	Young's modulus
f	Frequency
Hz	Hertz
m	Mass
Pa	Pascal
k	Spring constant
Q	Quality Factor
R	Resistivity
T	Temperature
V	Voltage
Q	Quality Facture
s	Second
V	Volt
W	Watt
°	Degree
L	Length

INTRODUCTION

Motivations of the study

The advent of Micro-electromechanical systems (MEMS) has brought about a revolutionary change in the domain of miniaturized devices. MEMS have the capacity to integrate mechanical and electrical components on a micro-scale single chip, thus making them highly desirable. MEMS have recently gained widespread attention due to their potential to serve in various applications, such as sensing, communication, and timing. MEMS resonators, which are integral constituents of several MEMS devices, play a crucial role in the overall functionality of MEMS systems.

Complementary Metal-Oxide-Semiconductor (CMOS) Micro-Electro-Mechanical Systems (MEMS) represent a groundbreaking class of micromachined systems that enable unparalleled levels of miniaturization and performance improvement by integrating MEMS devices with CMOS circuitry on a single chip. The term "CMOS MEMS" refers to both the integrated devices and the microfabrication technologies and processes needed to produce them.

The fabrication of CMOS MEMS devices involves the incorporation of MEMS transducers, such as accelerometers, gyroscopes, and microphones, with CMOS signal processing and control circuitry on the same substrate, resulting in highly integrated, multifunctional microsystems. Advanced semiconductor processing techniques, such as lithography, deposition, etching, and doping, are typically used to fabricate these devices. Furthermore, specialized post-processing steps, such as wafer bonding and release, are often necessary to enable their functionality, as depicted in Figure 0.1.

The development of CMOS MEMS technology has presented new possibilities for creating highly efficient, low-power, and cost-effective microsystems with a wide range of applications in various fields, including biomedicine, aerospace, consumer electronics, and industrial automation.

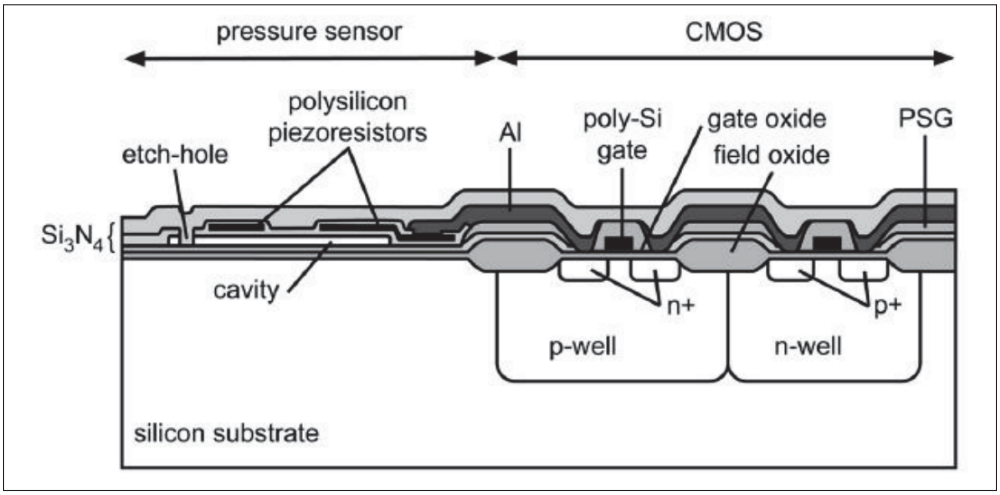

Figure 0.1 [Schematic illustration of a pressure sensor consisting of a silicon nitride membrane structure with embedded piezoresistors made of polysilicon. Taken from Kumar Mishra *et al.* (2021)

Microelectromechanical systems (MEMS) that tightly couple CMOS electronics and micro-mechanical structures are MEMS resonators. These devices, which are miniature mechanical devices vibrating at a specific frequency in the range of a few kilohertz to several megahertz, have been gaining significant attention in various applications, such as sensing, filtering, and timing. MEMS resonators are highly valued for their small size, low power consumption, and high reliability, making them a promising alternative to traditional quartz crystal resonators, which are much larger. Notably, MEMS-based oscillators are widely used to generate stable signals at a specific frequency, and they are highly stable, consume less power, and have a much smaller form factor than their quartz-based counterparts.

The market for MEMS resonators is projected to experience significant growth in the upcoming years. As per the report by MarketsandMarkets, the MEMS market is anticipated to reach a value of $11.7B by 2025, exhibiting a compound annual growth rate (CAGR) of 7.4% between 2019 to 2025, as illustrated in Figure 0.2. This growth is attributed to the increasing demand for miniature, low-power devices in a range of industries, such as automotive, healthcare,

and consumer electronics, as depicted in Figure 0.3. Given the extensive applications of MEMS resonators and their potential for further market growth, it is essential to investigate them meticulously. Researchers should strive to comprehend the fundamental principles of MEMS resonators, including their mechanical properties, resonant frequencies, and damping mechanisms. Moreover, they should explore novel applications of MEMS resonators and develop innovative designs to fulfill the evolving demands of various industries. By studying MEMS resonators, researchers can contribute to the development of innovative technologies and applications that will shape the future of electronics and communication systems. Importantly, this research can help mitigate weaknesses of MEMS resonators in order to democratize their use instead of established conventional technologies such as quartz crystal.

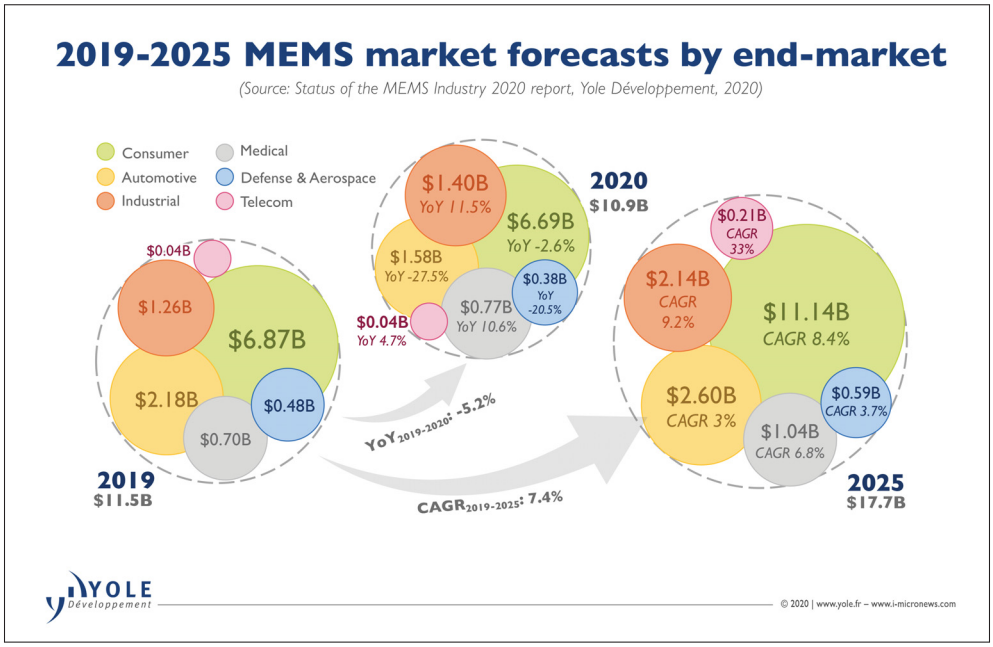

Figure 0.2 Applications of MEMS resonators in different industries
Taken from Développement

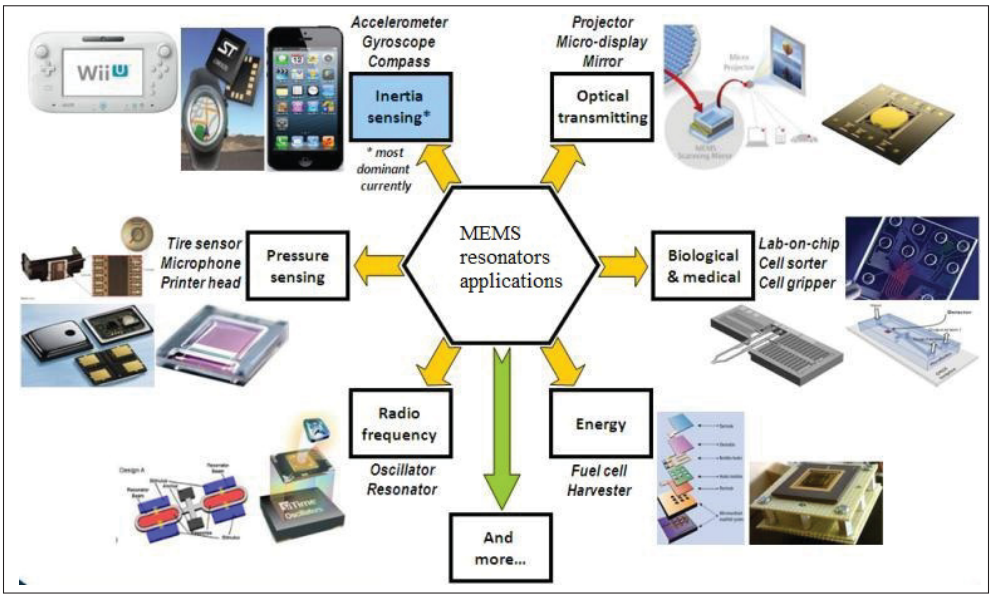

Figure 0.3 The forecast of MEMS market growth
Taken from Liu *et al.* (2013)

Research Problem

One of the principal challenges in the development of MEMS resonators is the minimization of energy damping and loss. Loss of energy in MEMS resonators can occur due to various mechanisms, including material damping, air damping, and anchor loss. Material damping is caused by the internal friction of the material and is typically proportional to the square of the frequency. Air damping is caused by the viscous drag of ambient air molecules on the surface of the resonator, and it is typically proportional to the resonator's surface area. Anchor loss is caused by the coupling of the resonator to the substrate or the packaging material, and it is typically proportional to the resonator size and the stiffness of the anchor. In order to improve the performance of MEMS resonators, it is essential to understand and quantify the damping mechanisms that limit their performance. Researchers have developed various techniques to mitigate energy damping, such as designing resonators with specific shapes and sizes, using novel materials, and optimizing the resonator's operating conditions. Additionally,

it is crucial to understand the effects of energy damping on the behavior of MEMS resonators, including changes in frequency, amplitude, and phase. By developing strategies to mitigate energy damping and minimize its effects, researchers can further improve the performance of MEMS resonators, enabling their use in a broader range of applications.

To mitigate energy damping and loss in MEMS resonators, various strategies have been proposed. One of the approaches is to employ low-loss materials such as diamond or single-crystal silicon for the resonator structure. These materials have high stiffness and low internal friction, resulting in lower energy dissipation. Another approach is to reduce air damping by employing vacuum packaging, which minimizes the effect of air molecules on the resonator surface. Additionally, anchor loss can be mitigated by using flexible anchors or suspending the resonator in the air, which reduces the stiffness of the anchor and lowers the coupling to the substrate. However, these methods have their own limitations and further investigation is required to develop more effective solutions that can address the limitations and tradeoffs between performance, manufacturability and cost.

Another critical challenge in MEMS resonators is achieving tunability. Typically, MEMS resonators are designed to resonate at a specific frequency, and modifying their resonant frequency post-fabrication is difficult. However, tunability is crucial in numerous applications such as frequency synthesizers and filters. Frequency tuning offers an efficient approach to counter frequency instability and enables smooth transitions between bistable states He, Feng, Roukes & Yang (2008). Moreover, it provides a promising avenue for achieving adjustable sensitivity Mei & Li (2013). Various approaches have been proposed to achieve tunability in MEMS resonators, including electrostatic tuning, piezoelectric tuning, and mechanical tuning. Importantly, achieving wide-ranging tunability post-fabrication can provide MEMS resonators with a significant advantage in comparison to quartz crystals which are known to be hard to tune post-fabrication. A few methods have been proposed to achieve MEMS resonator resonant

frequency tuning. Electrostatic tuning involves applying a voltage to the resonator electrodes to alter the effective stiffness of the resonator. Piezoelectric tuning involves applying mechanical stress to the resonator using piezoelectric materials to change its resonant frequency. Mechanical tuning involves changing the geometry of the resonator, such as its length or width, to adjust its resonant frequency. While these approaches have shown promising results, but they also have limitations, such as limited tunability range, complex post-processing, irreversible tuning, and significant power consumption requirements. The resonant frequency can be tuned through two distinct methods: analog and digital tuning. Analog tuning provides the advantage of fine-tuning and precise frequency selection within the tuning range. On the other hand, digital tuning offers its own set of advantages. Specifically, in DDS (Direct Digital Synthesis) devices, digital tuning enables swift switching between output frequencies and the ability to operate over a broad frequency spectrum, thanks to its inherently digital (or discrete) nature. These benefits serve as the primary motivation for the current research, as it focuses on studying the mechanisms and benefits of digital tuning.

In summary, MEMS resonators have demonstrated immense potential for various applications, but numerous research challenges and needs must be addressed to increase their use and become the dominating timing technology. Energy damping and loss reduction and tunability are two critical areas that require further research to fully utilize the potential of MEMS resonators. Addressing these research challenges and needs will enable the development of more efficient and reliable MEMS resonators for various applications.

Research objectives

This thesis presents the culmination of three years of research focused on the design, fabrication, and characterization of clamped-clamped beam resonators for the reduction of anchor loss and the creation of tunable resonators.

In this thesis, two critical challenges facing MEMS resonators in timing applications are focused on: anchor energy loss reduction and frequency tunability. Firstly, a method to mitigate the anchor energy loss using arrays of holes on the anchoring structure is proposed. Secondly, a novel frequency-tuning method, using electrostatic actuators, is proposed and its efficacy in achieving frequency tunability is assessed.

The results of this thesis provide a comprehensive understanding of the fundamental principles governing MEMS resonators and highlight the importance of meticulous design and characterization in achieving superior performance. This research tries to make a significant contribution to the field of MEMS resonator design, offering valuable guidance to researchers and designers seeking to optimize these devices for timing applications by improving their quality factors and their frequency agility.

Contributions

The main contributions of this thesis, embodied in two submitted journal papers, are as follows:

1. **A 2D numerical model to predict the anchor loss by estimation of the energy loss through the anchors in the form of wave propagation loss**

   To reduce anchor loss and improve the quality factor of MEMS resonators, a novel design approach utilizing trenched holes on the anchoring structure is proposed. A numerical analysis is conducted to evaluate the effectiveness of this design, followed by experimental validation using a set of 25 devices. The results demonstrate the efficacy of this approach in reducing anchor loss and improving the performance of MEMS resonators.

2. **A novel design to make a beam resonator's frequency tunable electrostatically over a relatively wide range**

To enhance the tunability of MEMS resonators, this study introduces a novel approach that involves electrostatically manipulating the anchoring structure and increasing the stiffness of the resonance structure. By doing so, the resonance frequency can be tuned. The proposed approach represents a significant contribution to the field of MEMS resonators and has the potential to facilitate the development of new technologies and applications that require frequency agile MEMS resonators.

Structure of the thesis

The present thesis is structured as follows, with the aim of providing a comprehensive account of the motivations, development, findings, and potential future directions of the research project:

- Chapter 1 provides a comprehensive literature review on MEMS resonators with the aim of providing an overview of their functionality and applications. The chapter also delves into the mechanisms of energy loss, such as material damping, air damping, and anchor loss, as well as the different tuning techniques used to manipulate the resonant frequency of MEMS resonators, including electrostatic tuning, piezoelectric tuning, and mechanical tuning. Through the examination of existing literature, this chapter provides a foundation for the subsequent chapters on the design and characterization of anchor loss reduction and tunable frequency MEMS resonators.

- Chapter 2.5 focuses on the modeling, design, and fabrication of clamped-clamped beam MEMS resonant devices, with a particular emphasis on anchor loss reduction. The chapter presents the impact of different shapes of energy reflector holes placed on the anchoring structure on the anchor loss and quality factor of the beam resonators. This chapter is based on the manuscript entitled "Anchor Loss Reduction in MEMS Flexural Beam Resonators Using Trench Hole Array Reflectors" submitted to the MDPI Micromachines journal.

- Chapter 2.5 introduces a tunable MEMS resonator, where two DC actuators with springs are employed to shift the frequency of clamped-clamped beam resonators by manipulating the anchors, leading to an increase in the spring stiffness of the anchors and, thus, the frequency of the resonator. The chapter highlights the structure operating principle and its potential for achieving high tunability of the resonant structure. This chapter is based on the manuscript entitled "Frequency Selection in a MEMS Flexural Beam Resonator by Electrostatic Actuation" submitted to the IEEE Journal of MEMS (JMEMS).

Finally, the thesis concludes with a summary of the outcomes of this work and a discussion of their implications. Additionally, potential future directions for further research and development are also addressed in this section.

CHAPTER 1

LITERATURE REVIEW

1.1 MEMS technology and devices

Micro-electromechanical systems (MEMS) are miniature-scale devices that combine mechanical and electrical parts, typically with dimensions ranging from a few micrometers to a few millimeters l'Encyclopædia Britannica. The development of MEMS technology emerged in the early 1970s to reduce power and material consumption, increase reproducibility, reduce the size of components and devices, and improve integration capabilities. MEMS technology is a multidisciplinary field that involves various areas of science and engineering, including material science, physics, and chemistry and requires a thorough understanding of mechanical and electrical phenomena.

The great number of applications and potentials of MEMS technology have lead to the development of many devices including but not limited to gyroscopes Zhang, Zhang, Chen & Li (2022), energy harvesters Chauhan, Joglekar & Manhas (2019); Chimeh, Nabavi, Al Janaideh & Zhang (2021); Nabavi, Aljaroudi & Zhang (2018); Toshiyoshi, Ju, Honma, Ji & Fujita (2019), accelerometers Varanis, Silva, Mereles & Pederiva (2018), wireless power transfer He, Liu, Yang, Wang, Chen & Yang (2014); Nabavi & Bhadra (2021), actuators Bell, Lu, Fleck & Spearing (2005); Conway, Traina & Kim (2007); Nabavi, Ménard & Nabki (2022); Takeshita, Nguyen, Daniel, Takei & Kobayashi (2022) and other devices. A number of MEMS based devices can be named as Mishra, Dubey, Mishra & Khan (2019): micro mirrors arrays and tunable mirrors, micro-machined ultrasound transducers, RF switches and tunable filters, microfluidic MEMS medical devices.

1.2 Fabrication of MEMS devices

In the last two decades, microfabrication processes have undergone significant advancements. The low-cost batch fabrication techniques of MEMS devices, which are similar to integrated

circuit manufacturing processes, along with their high potential for high-level integration with other microelectronics on the same package, have rendered them suitable for various applications Partridge, Lee, Hagelin & Menon (2013). The fabrication processes for Microelectromechanical systems can be divided into two main categories: surface and bulk micromachining. Surface micromachining is employed when devices can be fabricated using the deposition and etching of thin layers of materials on top of a substrate Bustillo, Howe & Muller (1998); Cai, Tan, Hua, Qin & Zhu (2018); Linder, Paratte, Grétillat, Jaecklin & De Rooij (1992). The typical surface micromachining steps are shown in Figure 1.1, showing the micromachining of a temperature sensor.

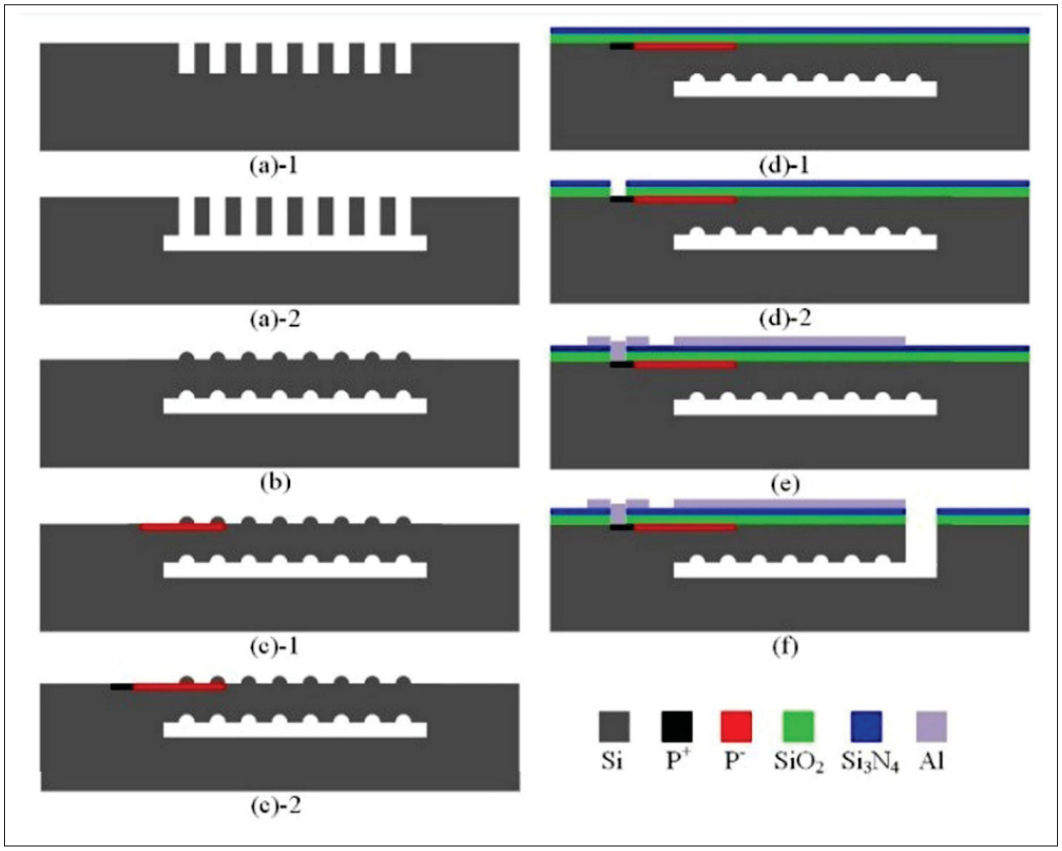

Figure 1.1 Steps involved in the surface silicon micromachining CMOS MEMS for in fabrication of miniature temperature sensors
Taken from Cai *et al.* (2018)

On the other hand, bulk microfabrication processes involve the etching of the substrate itself Kovacs, Maluf & Petersen (1998). Wet anisotropic etching is a commonly used technique in silicon bulk micromachining to produce microstructures for diverse applications within the field of MEMS. It is also extensively utilized to create surface texturing that reduces light reflectance and enhances the efficiency of crystalline silicon solar cells. In wet bulk micromachining, the etch rate is a crucial factor that affects the overall throughput Pal, Swarnalatha, Rao, Pandey, Tanaka & Sato (2021); Zou, Wang & Li (2017). Figure 1.2 illustrates the steps involved in the fabrication of a thin-film under bulk (TUB) using bulk micromachining process Zou *et al.* (2017).

In most cases, these two fabrication processes are combined together, where the MEMS fabrication process consists of one or more deposition processes, mainly including but not limited to low-pressure chemical vapor deposition (LPCVD) (Hersee & Duchemin (1982)), DC magnetron deposition (Reicher, Christian, Davidson & Peplinski (2009)), dry etch (Rangelow (2001)) and wet etch (Pal & Sato (2017)).

1.3 MEMS resonators

Microelectromechanical systems (MEMS) resonators are miniaturized mechanical components that use vibration to filter a signal. They are used in a variety of applications such as timing (Ng, Yang, Hong, Ahn, Heinz, Flader, Chen, Everhart, Kim, Melamud et al. (2015); Wu, Xu, Ng & Chen (2020)), frequency control (Kim, Melamud, Candler, Hopcroft, Jha, Chandorkar & Kenny (2010)) and sensing (Zhao, Montaseri, Wood, Pu, Seshia & Kraft (2016)).

MEMS resonators have gained increasing attention in the field of frequency control for electronic devices due to their small size, low power consumption, and high reliability Nguyen (2007). The resonators consist of a thin membrane that is supported by a substrate, which is excited at its resonant frequency to produce a vibration that is converted into an electrical signal to control the frequency of the device. MEMS resonators offer several advantages, including their ability to be accurately tuned to a specific frequency, making them ideal for high-precision timing

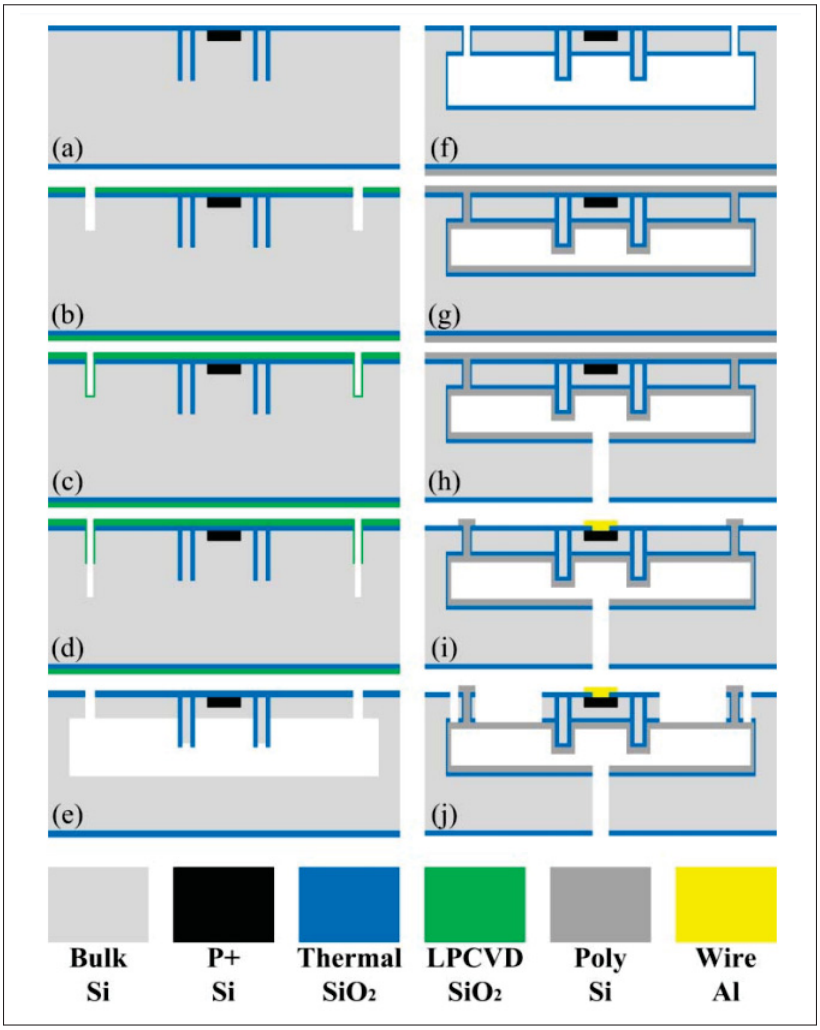

Figure 1.2 Bulk microfabrication process for the implementation of differential pressure sensors
Taken from Zou *et al.* (2017)

and frequency control applications. Moreover, their small size allows them to be integrated into a variety of small form factor devices, such as watches, smartphones, and medical devices. Furthermore, MEMS resonators have high-frequency stability, owing to the stability of the resonance frequency of the membrane Kim, Candler, Hopcroft, Agarwal, Park & Kenny (2007).

Overall, MEMS resonators are a promising option for frequency control in various applications due to their small size, low power consumption, high reliability, and the ability to be tuned to a

wide range of frequencies Campanella, Narducci, Merugu & Singh (2017); Weinstein, Bhave, Tada, Mitarai, Morita & Ikeda (2007).

1.3.1 Equivalent electrical circuit representation

Figure 1.3 presents an electrical model that provides an equivalent representation of a microresonator with electrostatic input and output ports. This model comprises an input transformer that converts an input voltage into a force and applies it to the mechanical system. The mechanical system is represented by a series RLC circuit. At the output port, another transformer is responsible for converting the velocities of the mechanical structure into an electrical current. It should be noted that analogous models can be developed for other transduction mechanisms, such as thermal or piezoelectric devices, taking into account the mechanisms involved in the conversion of the electrical signal to a mechanical one and vice versa.

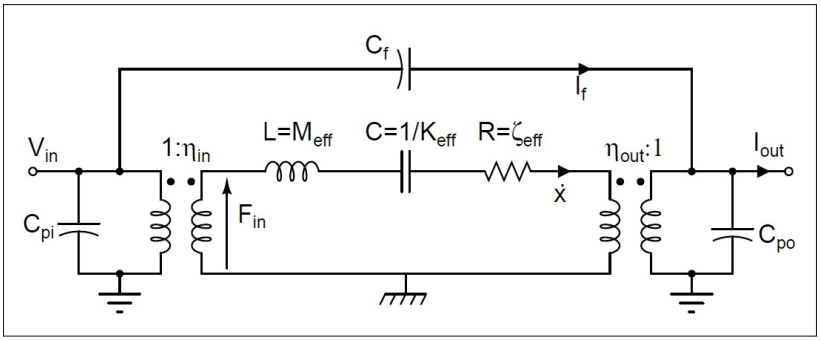

Figure 1.3 Representation of the equivalent electrical circuit of an electrostatic resonator, showing the electromechanical coupling coefficients (η_{in}) and (η_{out}), feedthrough capacitor (C_f), and parasitic capacitors (C_{pi} and (C_{p0})).
Taken from Abdolvand *et al.* (2016)

1.4 Quality factor

The quality factor (Q) of a MEMS resonator is a measure of its energy storage and dissipation characteristics. It is defined as the ratio of the energy stored in the resonator to the energy lost

from it during each cycle. Hence, the Q can be expressed as Tilmans, Elwenspoek & Fluitman (1992)

$$Q = 2\pi \frac{W}{\Delta W} \tag{1.1}$$

where ΔW is the dissipated energy per each vibration cycle and W is the maximum stored energy in the resonator structure in each cycle, respectively. A higher Q indicates that more energy is stored in the resonator, resulting in a higher Q. High Q is desirable for MEMS resonators because they lead to improved stability and accuracy Bajpai & Zaghloul (2009) and better signal-to-noise ratios Fadel, Dufour, Lochon & Francais (2004).

Various factors contribute to the dissipation of energy in a resonating system. The total energy loss of a resonator is influenced by the reciprocal summation of the Q of all the energy loss mechanisms Yasumura, Stowe, Chow, Pfafman, Kenny, Stipe & Rugar (2000)

$$\frac{1}{Q_{total}} = \frac{1}{Q_{air}} + \frac{1}{Q_{anchor}} + \frac{1}{Q_{surface}} + \frac{1}{Q_{TED}} + \frac{1}{Q_{others}} \tag{1.2}$$

1.5 Energy loss mechanisms

Damping is a crucial aspect in the design and optimization of microelectromechanical systems (MEMS)-based sensors and actuators. The quality factor, or Q, is a prevalent metric that characterizes the energy dissipation resulting from damping in such systems. Accurately measuring the damping present in a vibrating structure and understanding its underlying physics enables one to increase the sensitivity of the device or sensor by strategically engineering the resonator to increase the Q. It is worth noting that the Q is directly related to the energy losses in the system, as described in recent studies such as Wang, Carcione, Ba, Alajmi & Qadrouh (2019).

1.5.1 Anchor losses

Anchor losses are a crucial factor that leads to energy dissipation in MEMS resonators, primarily due to the mechanical connections that suspend the resonator to a supporting frame. These losses result from complex radiation phenomena occurring in a semi-infinite elastic half-space and often remain poorly understood Rodriguez, Chandorkar, Glaze, Gerrard, Chen, Heinz, Flader & Kenny (2018). The elastic waves that get trapped leak through the connections and propagate to the frame, leading to a considerable loss of energy. The extent of energy loss depends on the size and location of the anchor, and analytical analysis and prediction of anchor loss can be challenging Hao, Erbil & Ayazi (2003). However, finite element models have become increasingly popular among designers to accurately capture anchor losses and reduce their impact on the system Siddiqi, Fedeli, Tu, Frangi & Lee (2019). These numerical methods allow for the precise simulation of the behavior of complex systems and enable accurate predictions of energy loss in resonator systems. Additionally, experimental techniques such as laser Doppler vibrometry and acoustic microscopy can be used to measure the energy loss in MEMS resonators Rodriguez, Gerrard, Glaze, Chandorkar, Comenecia, Chen, Flader & Kenny (2017).

Effective management of anchor losses is crucial for improving the Q of MEMS resonators, as anchor losses can significantly decrease the resonator's energy storage capacity. Other factors that contribute to energy loss in MEMS resonators and reduce the Q include viscous damping, thermoelastic damping, and clamping losses. To enhance the performance and efficiency of MEMS resonator systems in various applications, such as sensors, oscillators, and filters, it is essential to identify and mitigate these sources of energy loss.

1.5.2 Viscous losses

In MEMS resonators, viscous loss or air damping is a prominent mechanism that leads to energy dissipation, resulting from the interaction between the resonator and the surrounding fluid or gas Dennis, Ahmed, Khir & Rabih (2015). The damping force arises due to the collision of air molecules with the resonator, causing a reduction in its vibrational amplitude. The

extent of the viscous loss is primarily dependent on the damping coefficient, which, in turn, is determined by various parameters such as the viscosity of the fluid, the size, and geometry of the resonator, and the frequency of its vibrations Alcheikh, Kosuru, Kazmi & Younis (2020). Proper characterization of the damping coefficient is essential for designing efficient MEMS resonator systems, particularly in applications that require high sensitivity and long-term stability Aoust, Levy, Bourgeteau & Le Traon (2015). Figure 1.4 illustrates the flow of streamlines around various cross sections of a rectangular thin beam, affected by viscous damping in the fluid. The visualization shows the fluid pattern surrounding the beam as it interacts with the surrounding medium. Understanding the underlying principles of viscous loss can also facilitate the development of advanced modeling and simulation techniques to predict and optimize the performance of MEMS resonators.

1.5.3 Thermoelastic losses

Thermoelastic damping is an energy loss mechanism that arises in MEMS resonators due to thermal and elastic energy coupling. It is a fundamental source of energy dissipation in MEMS resonators, and its effects on the system's performance can be especially significant at high frequencies. The damping resulting from thermoelastic effects can lead to reduced Q and a decreased energy storage capacity of the resonator. Therefore, identifying, understanding, and minimizing the impact of thermoelastic damping is crucial for enhancing the efficiency and sensitivity of MEMS resonators. (Khisaeva & Ostoja-Starzewski (2006); Schiwietz, Weig & Degenfeld-Schonburg (2022)).

Thermoelastic damping in vibrating structures is a fundamental contribution to the field of MEMS. Zener (1937) derived general expressions for thermoelastic damping, which he applied to the specific case of a beam in its fundamental flexural mode. His calculations were based on fundamental thermodynamic expressions for stored mechanical energy, work, and thermal energy, which used coupled thermal-mechanical constitutive relations for stress, strain, entropy, and temperature. Despite the complexity of the calculations, Zener proposed a simplified approach to evaluate the energy expressions for a specific resonator. He used uncoupled dynamical equations

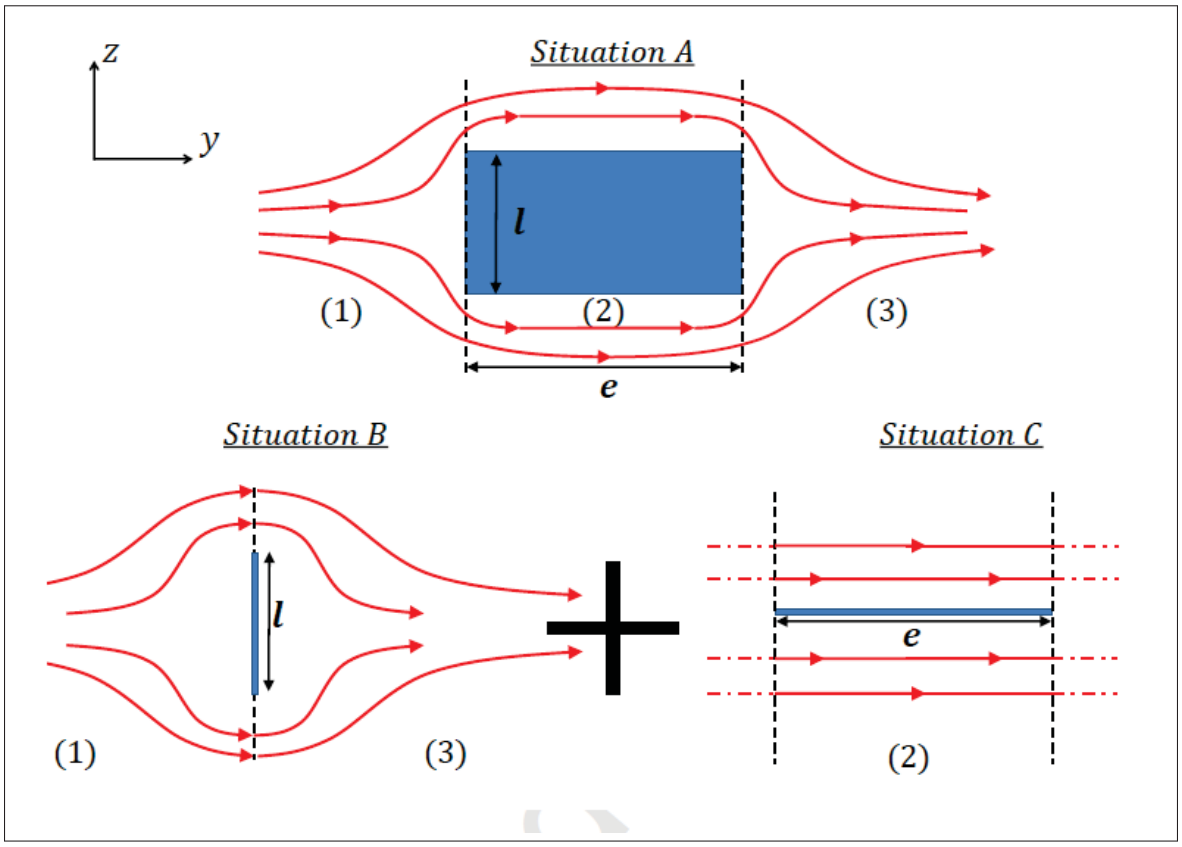

Figure 1.4 Diagram showing the streamlines of the incompressible fluid around a section of an oscillating cantilever beam in the fluid
Taken from Aoust *et al.* (2015)

to obtain the strain and temperature solutions and found the eigensolutions of the mechanical and thermal equations separately. By applying these to the coupled thermodynamic energies, Zener calculated the thermoelastic damping of an isotropic homogenous resonator as Zener (1938) :

$$\frac{1}{Q} = \left(\frac{E\alpha^2 T}{C_v}\right) \sum_n \frac{\omega_{mech}\tau_n f_n}{1 + (\omega_{mech}\tau_n)^2} \,, \tag{1.3}$$

where ω_{mech} is the mechanical resonance frequency and τ_n is the characteristic time constant of a given thermal mode. f_0, is the weighting function of a given mode, n. Although Zener's approach may seem simplistic, it is a powerful tool for predicting the damping behavior of

MEMS resonators. His work has been the foundation for subsequent studies on thermoelastic damping, and his analytical expressions remain relevant to this day.

The size and geometry of MEMS resonators have been extensively studied in relation to their impact on thermoelastic energy loss (Sorenson & Ayazi (2014); Yi (2008,0,0); Zhang, Kim, Choi & Cho (2016)). Geometric manipulation has been employed by some researchers as a means of reducing thermoelastic energy dissipation and increasing the Q. For example, Candler, Duwel, Varghese, Chandorkar, Hopcroft, Park, Kim, Yama, Partridge, Lutz et al. (2006) demonstrated a decrease in thermoelastic energy loss by modifying the thermal-mechanical coupling through the introduction of machined slots into the beam resonator in sections of high strain. In another study, Cassella & Piazza (2016) proposed the use of thick AlN layers in contour mode MEMS resonators, in order to reduce the thermoelastic damping, and proved that this technique can lead to %72 increase in the Q.

1.6 Quality factor enhancement

Enhancing the Q of MEMS resonators is of significant interest in the field of microelectromechanical systems. Several techniques have been employed to enhance the Q of MEMS resonators, including reducing the thermoelastic damping (Duwel, Candler, Kenny & Varghese (2006)), and anchor loss reduction (Duwel *et al.* (2006)). The studied mechanisms to reduce the anchor loss in MEMS resonators is vastly discussed in the introduction of Chapter 2.5 of this thesis.

1.7 Transduction systems

MEMS resonators are frequently used in tandem with electronic circuits, necessitating the conversion of mechanical vibrations to electrical signals and vice versa. The efficacy of a resonator-containing device is largely determined by the method by which this energy conversion occurs, referred to as the transduction mechanism. When selecting a transduction mechanism, factors such as efficiency, simplicity, and power consumption must be taken into careful consideration. This section will explore two widely employed transduction systems.

1.7.1 Electrostatic transduction

Electrostatic transduction is a frequently employed technique in MEMS resonators for the conversion of electrical signals into mechanical vibrations and vice versa Agarwal, Park, Candler, Kim, Hopcroft, Chandorkar, Jha, Melamud, Kenny & Murmann (2006); Alsaleem & Younis (2010). This process leverages electrostatic forces to induce mechanical motion and to sense the displacement of the resonator Sridaran & Bhave (2011). The incorporation of electrostatic transducers is relatively simple, as they do not require specialized materials, except for high electrical conductivity for the electrode plates. This approach offers a broad range of movement and high sensitivity, rendering it suitable for use in high-frequency resonators Lim, Karacolak, Jiang, Huang & Zhao (2015). Nonetheless, electrostatic transduction is susceptible to environmental disturbances such as humidity and temperature, which may adversely impact the resonator's performance. Despite these challenges, electrostatic transduction remains a favored choice for MEMS resonators due to its versatility, near zero power consumption, and ease of implementation Sutagundar, Sheeparamatti & Jangamshetti (2014).

An important principle in MEMS resonator design is the use of capacitive transduction to convert electrical signals into mechanical vibrations and vice versa. This transduction method involves the application of a voltage between two conductive plates separated by an insulating medium, which generates a force that can cause one of the plates to move if it is free to do so. Conversely, if a constant voltage is supplied to the capacitor's conducting plates, a change in capacitance due to the movement will produce an electric current Chuang, Lee, Chang & Hu (2010). To optimize energy coupling in MEMS resonators, designers have explored various methods Gong & Piazza (2012); Hajjaj, Hafiz & Younis (2017a). Despite being widely used, electrostatically actuated MEMS resonators have limited power handling capability due to the presence of nonlinear effects in the material properties Zuo, Rinaldi & Piazza (2009).

1.7.2 Piezoelectric transduction

As an alternative to achieving decreased motional impediment, piezoelectric transduction makes use of advancements in the growth of piezoelectric thin films, such as thin film bulk acoustic resonators (FBARs). Piezoelectric resonators function through the conversion of mechanical stress which is caused by the electric polarization of piezoelectric materials (Trolier-McKinstry & Muralt (2004)). AlN, ZnO, and PZT are the most widely-reported piezoelectric thin films that have been applied to MEMS resonators (Bian, Jin, Wang, Dong, Chen, Luo, Deen & Qi (2015); Deshpande, Pande & Patrikar (2020); Hung & Nguyen (2011); Karabalin, Matheny, Feng, Defaÿ, Le Rhun, Marcoux, Hentz, Andreucci & Roukes (2009); Loebl, Klee, Metzmacher, Brand, Milsom & Lok (2003); Molarius, Kaitila, Pensala & Ylilammi (2003); Piazza, Felmetsger, Muralt, Olsson III & Ruby (2012)). In piezoelectric resonators, a ground electrode is positioned at the bottom, while alternating current voltage is applied to the top electrodes, generating an electric field that travels through the AlN structure. Typically, these resonators are designed to oscillate in the lateral direction, with their resonant frequency determined by the lateral geometry of the resonator. In certain investigations, a piezoelectric film has been incorporated onto a thick substrate layer to develop a piezoelectric resonator. Piezoelectric microbeam resonators are considered attractive when compared to electrostatically actuated resonators, primarily because they have the potential for lower insertion loss, especially at higher frequencies DeVoe (2001).

1.8 Resonance mode shapes

MEMS resonators are capable of exhibiting different modes depending on their design. These modes can be classified into several types including flexural modes, longitudinal modes, rotational modes, bulk modes, and acoustic modes Pillai & Li (2020); Platz & Schmid (2019). Flexural modes are commonly utilized in micro-scale devices and result from the bending of the structure Lin (1996). Longitudinal modes, on the other hand, involve the stretching and compression of the structure Kaajakari, Mattila, Lipsanen & Oja (2005). Rotational modes occur due to the twisting of the structure and are implemented in gyroscopes and other sensing applications Lipiäinen, Jaakkola, Kokkonen & Kaivola (2012). Lastly, acoustic modes arise from the vibration of a

thin membrane and find use in microphones and other audio-based applications Wang, Wang, Wang, Quan, Keshavarz, Madeira, Zhang, Wang & Kraft (2022). Here, we take a look at the most common vibration modes in MEMS resonators:

1.8.1 Bulk mode

Bulk mode operation of resonators is characterized by standing longitudinal waves Chandorkar, Agarwal, Melamud, Candler, Goodson & Kenny (2008). Bulk mode resonators are favored for higher frequency applications due to their efficient frequency-to-size scaling characteristic Li, Wen, Wisher, Norouzpour-Shirazi, Lei, Chen & Ayazi (2019); Matsumoto, Kadota & Tanaka (2020); Mccann, Mcgann, Parks, Frankel, Da Cunha & Vetelino (2009) as they are much stiffer than flexural mode resonators of the same physical dimensions, which translates to higher frequencies. Examples of bulk mode resonators, with their respective mode shapes, are shown in Figure 1.5. These resonators create longitudinal standing waves, whereby each part of the structure undergoes either compression or expansion, with the exception of the center, which is clamped to minimize losses. Piezoelectric resonators often operate using lateral bulk modes, specifically contour modes, in which acoustic radiation patterns are viewed as contours in the plane of fabrication. This stands in contrast to the thickness vibration modes of devices like the film bulk acoustic resonator (FBAR). Bulk-mode resonators offer the benefit of significantly higher Q and energy storage compared to flexural resonators. (Kaajakari *et al.* (2005); Mattila, Kiihamäki, Lamminmäki, Jaakkola, Rantakari, Oja, Seppä, Kattelus & Tittonen (2002); Shao, Palaniapan, Khine & Tan (2008); Zhu, Shan, Shek & Lee (2012))

1.8.2 Flexural mode

Flexural mode vibration is a prevalent type of mechanical vibration that can manifest in resonators. In this mode, the resonator experiences bending or flexing in response to an applied force or electrical signal, leading to the development of vibration at a specific frequency, which is determined by the resonator's physical properties, such as its geometry and material composition Tiwari & Candler (2019). In the realm of MEMS, flexural mode vibration is commonly used to

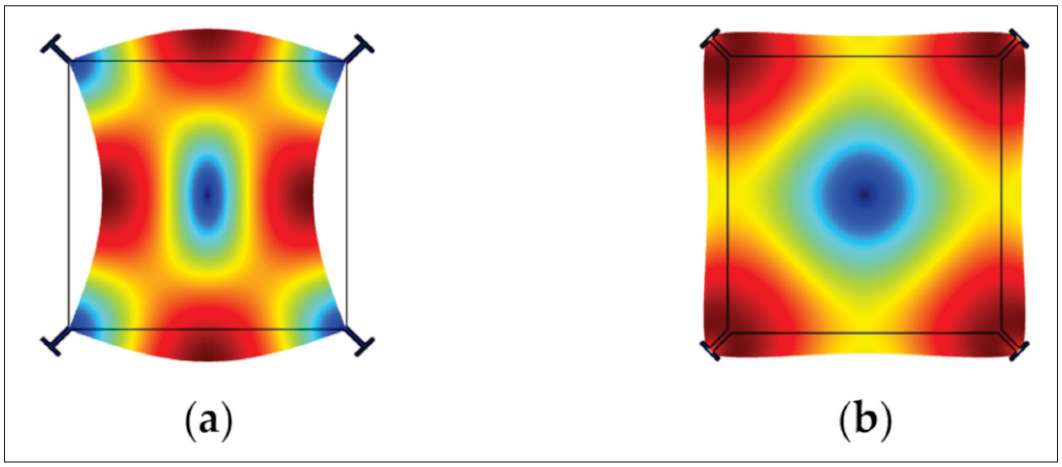

Figure 1.5 FEM simulation of (a) WG mode; (b) Extensional mode bulk acoustic wave (BAW) resonator in COMSOL
Taken from Wang *et al.* (2022)

operate resonators Puder, Bedair, Pulskamp, Rudy, Polcawich & Bhave (2015); Rudy, Pulskamp, Bedair, Puder & Polcawich (2016); Thakar, Wu, Peczalski & Rais-Zadeh (2013). In these structures, upon application of an electrical signal, the resonator experiences bending and flexing, resulting in the development of a vibrational mode that can be employed in sensing or signal processing applications. Figure 1.6 shows that compressive stress occurs in regions of the structure experiencing inward bending, while tensile stress is observed in areas undergoing outward bending.

1.8.3 Torsional mode

Torsional vibration is a type of angular vibration that arises due to the application of non-smooth or alternating torques at a distance from the rotational axis. The primary mode of movement associated with torsional vibration is rotational displacement, and the dominant form of stress experienced by the structure is shear stress. The paddle resonator is a commonly used torsional mode resonator in MEMS resonators. This device typically consists of a plate or disk that is axially supported by pairs of tethers, with the torsional movement of the supporting beams inducing vibrational motion in the resonant structure Yang, Ladhane, Wang, Lee, Young & Feng

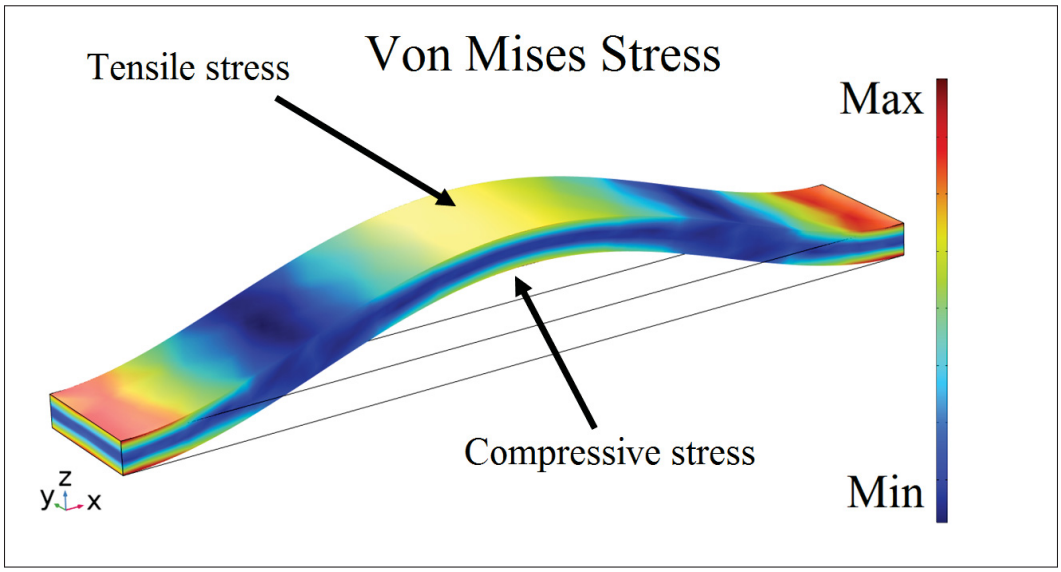

Figure 1.6 Stress distribution visualization in the flexural vibration mode of a clamped-clamped beam resonator

(2014); Yang, Zorman & Feng (2015). Figure 1.7 depicts the torsional mode resonators with both disk and plate shape resonators.

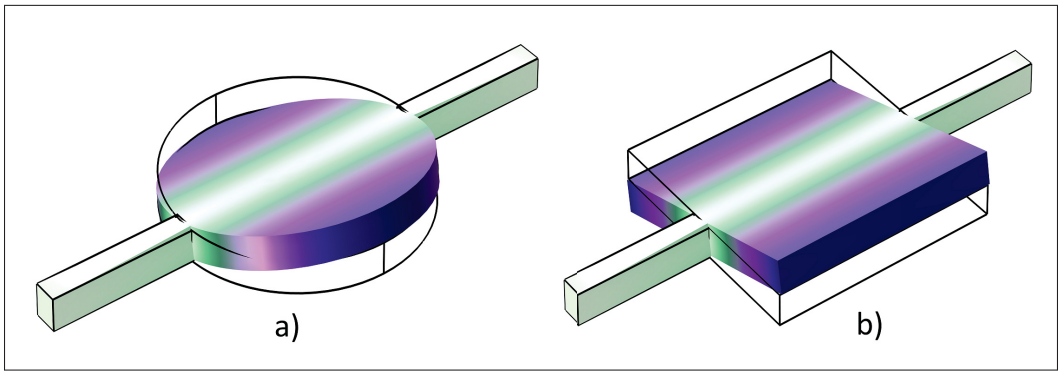

Figure 1.7 Torsional mode paddle a) disk and b) plate resonators

1.9 Frequency Tuning Mechanisms

Frequency tuning is a crucial aspect of MEMS resonator design as it enables optimization of the resonator's performance in various applications. The resonant frequency of a MEMS resonator directly impacts its performance in applications such as timing where the resonator frequency

determines the frequency of the generated clock signal. Therefore, precise control over the resonant frequency is necessary to ensure the accuracy and stability of the clock signal Serrano, Tabrizian & Ayazi (2011).

Moreover, external factors like temperature changes and mechanical stress can affect the resonant frequency of the resonator Melamud, Hopcroft, Jha, Kim, Chandorkar, Candler & Kenny (2005). By tuning the resonant frequency, it is possible to compensate for these external factors and maintain the desired performance and accuracy of the resonator Lavasani, Pan, Harrington, Abdolvand & Ayazi (2012). Several methods of frequency tuning are electrothermal, electrostatic, piezoelectric tuning and mass tuning Azizi, Ghazavi, Rezazadeh, Ahmadian & Cetinkaya (2014); Chang, Wei & Lee (2020); Chellasivalingam, Graves, Boies & Seshia (2020); Ibrahim & Ali (2012); Zhang, Hu, Peng & Meng (2015). Here, we talk about the most common tuning mechanism in MEMS resonators, i.e., electrothermal and electrostatic tuning.

A specific need for digital frequency tuning and frequency selection in resonators arises from the need to fulfill the demands of broader frequency coverage (Dubuc, Grenier & Iannacci (2018)). While existing cutting-edge MEMS resonators have demonstrated exceptional capabilities, they predominantly offer a singular frequency output. In communications, the deployment of filters centered on single-frequency resonators necessitates complex devices integrated with individual RF switches. This not only leads to a significant spatial footprint but also results in increased power consumption (Nguyen (1999)). Additionally, oscillators with single-frequency resonators often need to be incorporated with phase lock loop (PLL) circuits to accommodate the requisites of multi-frequency output, which inevitably makes the circuit control more complex and increases the phase noise (Loops (1996)). Accordingly, agile resonators with wide tuning ranges are of interest to simplify systems, and make them reconfigurable.

1.9.1 Electrohermal tuning

Electrothermal tuning involves physically changing the resonator's shape or size by changing its temperature, resulting in expansion or contraction phenomena that ultimately manifest as a shift

in its resonant frequency Verbridge, Shapiro, Craighead & Parpia (2007). Numerous studies have substantiated the efficacy of thermal actuators in the manipulation of resonator frequency, showcasing their ability to effectively decrease or augment the resonant frequency **?????**.

In previous studies, Zhang, Zhao, Xu, Jiang, Zhao, Wang & Liu (2013) and Svilicic, Mastropaolo, Flynn & Cheung (2012) explored the utilization of electrothermally induced stress for tuning the resonant frequency, achieving frequency tuning percentages of 0.34% and 9.7%, respectively. Similarly, Hajjaj, Ramini, Alcheikh & Younis (2017b) reported a significant frequency tuning of 168%. Additionally, Basirico & Lanzara (2012) demonstrated that altering the shape and inducing axial deformation of a structure can also impact its resonant frequency. Researchers have employed thermally induced buckling to tune the resonant frequency of clamped-clamped resonators, employing different buckling orientations and profiles Cao & Sepúlveda (2019). Guzman, Dinh, Phan, Joy, Qamar, Bahreyni, Zhu, Rais-Zadeh, Li, Nguyen et al. (2020) addressed the issue of thermal expansion mismatch in MEMS resonators by utilizing a single material for both the resonator and the heating element, thereby mitigating the drawback. In another study, Göktaş & Zaghloul (2014) incorporated embedded heaters to induce thermal axial loads on double-ended fixed beam resonators, resulting in a substantial frequency tuning ranging from 35.7% to 42.6%. Electrothermal tuning offer several benefits. They allow for a wide tuning range due to their ability to induce significant changes in the resonator's physical dimensions through thermal expansion or contraction Guzman *et al.* (2020). Additionally, electrothermal tuning is relatively straightforward to implement, as it typically involves the application of electrical current or voltage to generate heat, making it compatible with standard MEMS fabrication processes. However, one disadvantage of electrothermal tuning is the relatively high power consumption associated with the heating process, which can limit its use in power-constrained applications. As electrothermal methods suffer from higher power consumption Göktaş & Zaghloul (2014), researchers also explored electrostatic methods as an alternative for reducing power consumption in the frequency tuning mechanism.

1.9.2 Electrostatic tuning

Electrostatic tuning, employs voltage application to change the resonant frequency by adjusting the mechanical stiffness of the resonator. This method was used for tuning frequency in micromachined composite resonators for temperature compensation Lee, Melamud, Kim, Hopcroft, Salvia & Kenny (2011). The researchers applied it to a flexural-mode composite resonator. Experimental results revealed a remarkable ±2.5-ppm stability over a wide temperature range of 90°C. These findings, presented in the paper, contribute valuable insights into the use of electrostatic tuning for temperature compensation in micromachined resonators.

The effect of an electrostatically induced axial force on frequency shifting in micro-tuning fork resonators was investigated by Wang, Huan, Pu & Wei (2018). Additionally, Alcheikh, Ramini, Hafiz & Younis (2017) examined the bi-directional tuning of the resonant frequency in in-plane clamped-guided microbeam resonators by applying electrostatic axial tensile and compressive forces. In the realm of nano-scaled devices, the utilization of mechanical axial forces by inducing substrate bending to induce tensile stress in clamped-clamped nanoresonators was explored by Verbridge *et al.* (2007). Work in Wang *et al.* (2018) also investigated the effect of an electrostatically induced axial force on frequency shifting and tuning in micro fork resonators.

The introduction section of chapter Chapter 2.5 of this thesis discusses the frequency tuning mechanisms in MEMS resonators in more detail.

1.10 Applications of MEMS resonators

MEMS resonators are used in a wide variety of applications. They are used in consumer electronics, automotive, industrial, communications, and medical applications (Jha (2008); Lutz, Partridge, Gupta, Buchan, Klaassen, McDonald & Petersen (2007b)). In consumer electronics, MEMS resonators are used in mobile phones, tablets, and other consumer devices to provide the timing signals necessary for the operation of the device. They are also used in automotive applications for the timing of engine control systems (Lutz, McDonald, Gupta, Partridge,

Dimpel & Petersen (2007a)) and in industrial applications for the precision timing of control systems and machine automation. In communications applications, MEMS resonators are used to provide precise timing for radios and other communication systems (Basu & Bhattacharyya (2011)). Additionally, MEMS resonators are used in medical applications such as blood pressure sensors (Eidi (2022)).

MEMS resonators are also used in military and aerospace applications (Sastry (2009)). They are used to provide precise timing for navigation and guidance systems, as well as for radar and communication systems (Jmai, Gahgouh & Gharsallah (2017)). MEMS resonators are also used in satellites and other space vehicles to provide the necessary timing signals for their operation (Herrera-May, Soler-Balcazar, Vázquez-Leal, Martínez-Castillo, Vigueras-Zuñiga & Aguilera-Cortés (2016); Pavithra, Sathya & Muruganand (2015)). The precision timing signals provided by MEMS resonators are also used in aircraft and missiles, allowing them to navigate accurately in hostile environments.

1.10.1 Sensing

MEMS resonator resonators have become a prominent sensing technology and have been utilized in various applications. In industrial settings, these resonators are frequently utilized to detect changes in pressure levels. The small size of MEMS resonators makes them ideal for use in compact devices, such as pressure sensors, which can be deployed in harsh and challenging environments. This characteristic of MEMS resonators makes them a promising technology for use in industries such as oil and gas, aerospace, and automotive. By employing MEMS resonators, accurate and reliable detection of pressure changes can be achieved, leading to improved safety and efficiency in various industrial processes.(Bruckner, Cimalla, Niebelschutz, Stephan, Tonisch, Ambacher & Hein (2007); Qaradaghi, Mahdavi, Kumar & Pourkamali (2016)). This can be used for monitoring machinery or for detecting leaks (Hajjam, Logan, Pandiyan & Pourkamali (2011); Xu, Chai, Wu, Han, Wai, Li, Yeo, Nijhof & Gu (2018)) or other disturbances in a manufacturing process. Banerji, Fernandez & Madrenas (2017) conducted a series of experiments to characterize the resonant pressure sensor with respect to its frequency

response, temperature sensitivity, and pressure sensitivity over the range of $-10\,^{\circ}\mathrm{C}$ to $85\,^{\circ}\mathrm{C}$ and 0.1 kPa to 100 kPa. The authors found that the resonant pressure sensor which is shown in Figure 1.8, had a frequency response of 500 Hz at atmospheric pressure and the temperature sensitivity of the resonance frequency was $0.3\,\mathrm{Hz}\,^{\circ}\mathrm{C}^{-1}$ and the pressure sensitivity of the pressure sensor was $0.1\,\mathrm{Hz\,mbar}^{-1}$.

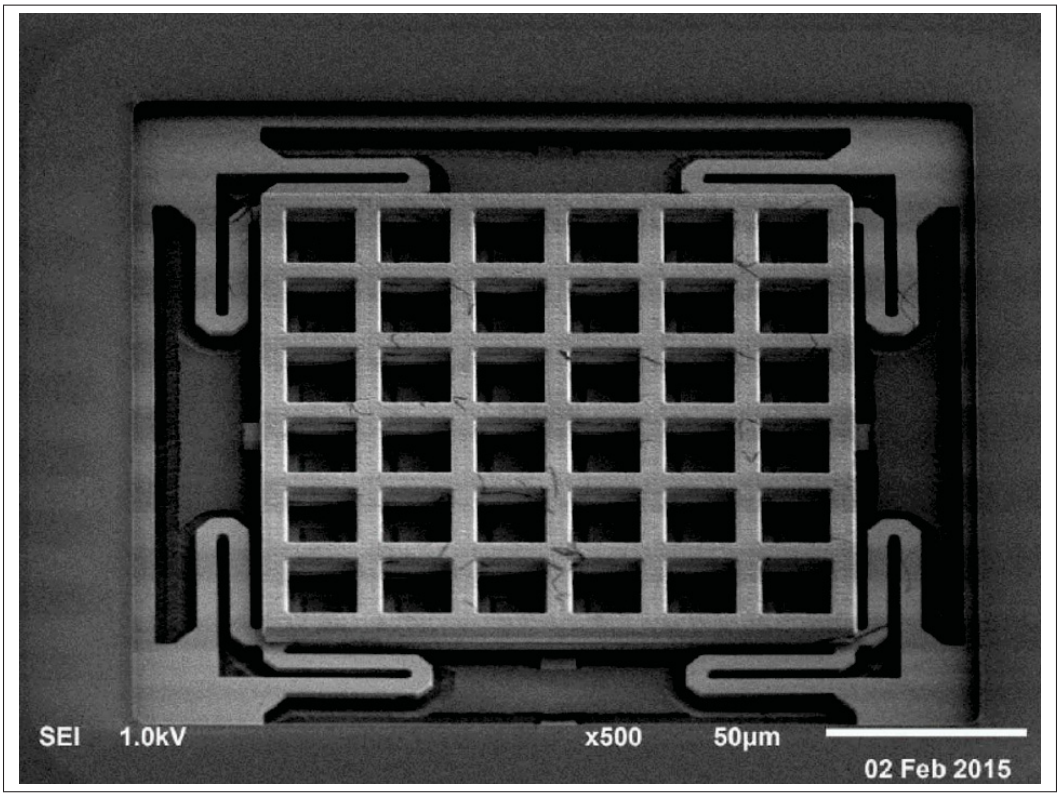

Figure 1.8 SEM of fabricated CMOS pressure sensor
Taken from Banerji *et al.* (2017)

MEMS resonators have gained considerable attention due to their ability to detect the mass of minute objects, including cells and particles, through the change in resonance frequency resulting from the mass loading effect. This mass-sensing methodology is gradually gaining significance in the scientific investigation and progress of diverse biomedical and biological applicatio (Pachkawade (2020)). MEMS cantilever resonators were fabricated by Davis, Svendsen & Boisen (2007) for mass sensing applications to measure masses down to the nanogram range.

In medical settings, they can be used for detecting changes in heart rate or respiration. Additionally, they can be used in consumer applications, such as for measuring acceleration in automotive applications (Tocchio, Caspani & Langfelder (2011); Zhao, Pandit, Sobreviela, Steinmann, Mustafazade, Zou & Seshia (2019)) and for measuring temperature (Campanella *et al.* (2017); Jha, Bahl, Melamud, Chandorkar, Hopcroft, Kim, Agarwal, Salvia, Mehta & Kenny (2007)) in home appliances.

1.10.2 Timing

In a timing application, a MEMS resonator is used to generate a stable oscillating signal with a specific frequency. This signal is then used as a reference for other circuits in the device, allowing them to operate at precise intervals and maintain synchronization (Hsu & Pai (2007); Lutz *et al.* (2007b)). For example, a MEMS resonator might be used to generate a clock signal that is used to control the timing of data transfer in a computer, or to generate a reference signal for a phase-locked loop circuit that is used to control the frequency of a radio transmitter.

Many applications require timing with highly stable frequency stability and MEMS resonators and MEMS-based oscillators are well-suited to timing applications because they can generate stable oscillating signals with very low jitter, which is the variation in the time between consecutive cycles of the oscillation (Lee, Partridge & Assaderaghi (2012); Melamud, Hagelin, Arft, Grosjean, Arumugam, Gupta, Hill, Lutz, Partridge & Assaderaghi (2012); Shahmohammadi, Modarres-Zadeh & Abdolvand (2010)). This allows them to maintain precise timing even in the presence of external noise or other sources of interference. In Figure 1.9 we can see the MEMS oscillator topology that focuses on the circuitry. This design incorporates a phase-locked loop (PLL) to convert the resonator frequency to meet the application's specific requirements. To adjust the resonator within production tolerances, a fractional PLL approach is utilized, and the multiplication value is usually variable to compensate for temperature variations. The state machine is responsible for controlling the PLL, which obtains its parameters from non-volatile memory.

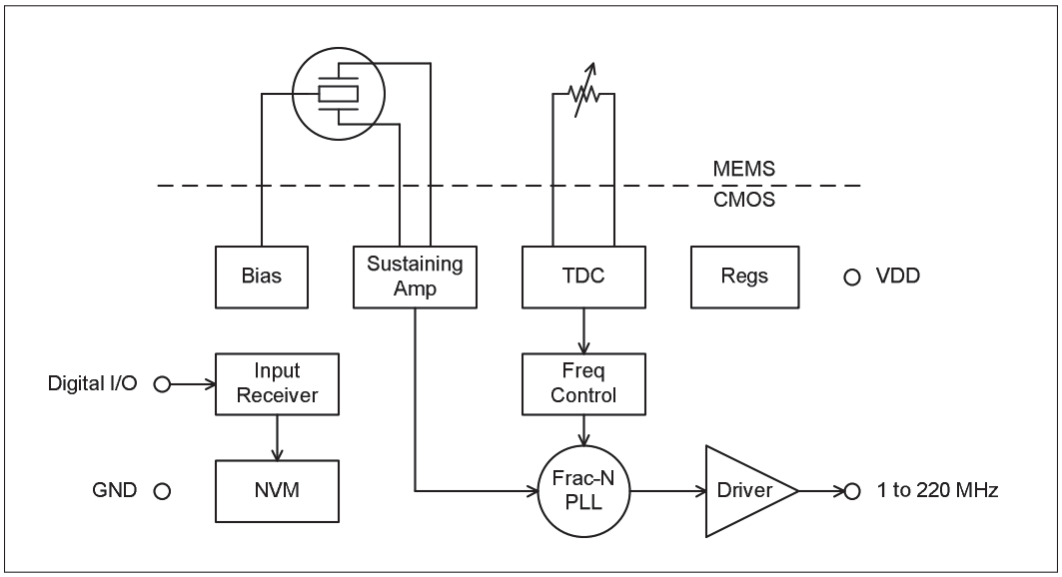

Figure 1.9 Oscillator topology, including phase locked loop (PLL)
Take from Banerji *et al.* (2017)

Additionally, because they are made using MEMS technology, they can be fabricated in very small sizes at low cost (Hsu (2007); Lutz *et al.* (2007b)), making them suitable for use in compact and portable devices. Wide range of timing applications, including smartphones (Lam (2016)), smart watches, and other portable devices, as well as in automotive (Lutz *et al.* (2007a)), and other applications.

1.11 Conclusion

In this chapter, a comprehensive review of the literature on MEMS technology and devices, including their fabrication and transduction systems, has been presented. The discussion has also focused on MEMS resonators, highlighting various resonance mode shapes, quality factors, and energy losses associated with these devices. The unique properties of MEMS resonators, such as their small size, low cost, and low power consumption, make them well-suited for a wide range of applications, including sensing and timing.

The resonant frequency of MEMS resonators is sensitive to various external factors, including temperature, pressure, and acceleration, which makes them suitable for sensing applications.

Moreover, the high-Q factors and low energy losses of MEMS resonators enable their use in timing applications, including frequency references for communication systems.

The primary aim of this thesis is to provide further insights into two critical aspects of MEMS resonators, namely, anchor loss reduction, and Q enhancement. A novel anchoring structure is proposed to reduce anchor loss, and the 2D wave propagation mode is introduced to validate the concept. Measurements are conducted on the fabricated resonators to demonstrate the feasibility of the proposed approach. In addition, in order to introduce multi-frequency resonators which, as discussed in section. 1.9, are needed in order to provide broad frequency coverage, reconfigurability and reduce the complexity and power consumption of communication devices, a new method for tuning the frequency of resonators using DC actuators to increase the stiffness of the resonator is investigated to increase the frequency. This study aims to contribute to the development of more efficient and precise MEMS resonators that can be used in a wide range of applications.

CHAPTER 2

ANCHOR LOSS REDUCTION IN MEMS FLEXURAL BEAM RESONATORS USING TRENCH HOLE ARRAY REFLECTORS

Mohammad Kazemi[1], Mathieu Gratuze[1], Seyedfakhreddin Nabavi[1], Frédéric Nabki[1]

[1] Département de Génie Électrique, École de Technologie Supérieure,
1100 Rue Notre-Dame Ouest, Montréal, Québec, H3C 1K3, Canada

Paper submitted to the IEEE Journal of Microelectromechanical Systems, April 2023

Abstract: The quality Factor of microelectromechanical resonators is a crucial performance metric and has thus been the subject of numerous studies aimed at maximizing its value by minimizing anchor loss. This work presents a study on the effect of elastic wave reflectors on the quality factor of MEMS clamped-clamped flexural beam resonators. The elastic wave reflectors are a series of holes created by trenches in the silicon substrate of the resonators. In this regard, four different shapes of arrayed holes are considered,i.e., two sizes of squares and two half circles with different directions are placed near the anchors. Their effect on the quality factor is surveyed numerically and experimentally. 2D in-plane wave propagation theory with a low-reflecting fixed boundary condition was used in the numerical simulation to predict the behavior, and the MEMS resonator prototypes were fabricated using a commercially available micro-fabrication process to validate the findings. It is found that the half-circle-shaped holes with their curved side facing the anchors have the best performance. With these reflectors, the quality factor of the resonator, in vacuum, is increased by a factor of 1.7× in air or 1.72× in vacuum. .

Keywords: Beam resonators, acoustic wave reflector, quality factor, anchor losses

2.1 Introduction

MEMS resonators have been used for a wide range of applications such as gas sensing Blue, Brown, Li, Bauer & Uttamchandani (2020); Weng, Pillai & Li (2020), frequency tracking Baù, Ferrari, Ferrari, Ali & Lee (2019), magnetic sensing Zhang, Wu, Sang, Wu, Huang, Wang, Takahashi, Li, Koizumi & Toda (2020) and thermo-humidity sensing Jaber, Ilyas, Shekhah, Eddaoudi & Younis (2018). The quality factor (Q) of a resonator is a crucial metric that quantifies the overall performance of the device. Q is a dimensionless parameter that describes the energy stored in the resonator divided by the energy lost per cycle, and can be expressed as Tilmans *et al.* (1992):

$$Q = 2\pi \frac{W}{\Delta W}, \tag{2.1}$$

where W and ΔW denote the maximum stored energy in the resonator structure and the dissipated energy during each vibration cycle, respectively. There are different mechanisms that lead to the dissipation of energy in a resonating system. The total Q of a resonator can be determined by the reciprocal summation of the Q of all of the energy loss mechanisms Yasumura *et al.* (2000) such that :

$$\frac{1}{Q_{total}} = \frac{1}{Q_{air}} + \frac{1}{Q_{TED}} + \frac{1}{Q_{surface}} + \frac{1}{Q_{anchor}} + \frac{1}{Q_{others}}. \tag{2.2}$$

Each term of equation 2.2 relates to an energy loss mechanism. Q_{air} denotes the air or viscous energy loss which occurs due to the compressive force of the peripheral medium (e.g., air) onto the surface of the resonator Alcheikh *et al.* (2020); Dennis *et al.* (2015), Q_{TED} is the thermo-elastic damping that is caused by the induced temperature gradient by the mechanical vibration of the resonator Kumar & Mukhopadhyay (2020); Segovia-Fernandez & Piazza (2017); Tai & Chen (2019), and $Q_{surface}$ is the surface loss that is caused by the existence of a thin layer of contaminations and defects on the surface of the resonator Gusso (2020). In addition, Akhiezer damping Kunal & Aluru (2011) is another source of energy loss in resonators comprehensively

studied by Rodriguez, Chandorkar, Watson, Glaze, Ahn, Ng, Yang & Kenny (2019). Finally, Q_{anchor} is due to the energy loss through the anchoring structures into the substrate, which is one of the main sources of energy loss in resonators Rodriguez *et al.* (2018).

In vacuum, where the air damping is diminished, the main energy losses occur through the anchors and thermo-elastic damping Rodriguez *et al.* (2017). Analytical modeling of the anchor loss has been extensively employed in order to minimize energy dissipation. Qualitative analytical and quantitative numerical methods were proposed by Segovia-Fernandez & Piazza (2016) to predict the anchor loss of AlN 65 MHz contour mode resonators considering the anchor as a 1D waveguide. A theoretical model for the anchor loss of flexural beam resonators with in-plane vibration was presented by Hao *et al.* (2003). The effect of different design parameters such as different electrode patterns, and also the curvature of the resonating structure's edges on the Q of AlN on silicon Lamé mode resonators were studied using the perfectly matched layer (PML) method by Siddiqi *et al.* (2019). Moreover, the effect of anchor geometry on the Q of width extensional mode resonators at 52 MHz were modelled in Gerrard, Ng, Ahn, Hong, Yang & Kenny (2015) using a PML. This work confirmed that the anchor geometry has a significant effect on the Q of these types of resonators. Notably, many other works have widely discussed analytical and numerical models, in order to predict the anchor loss and Q of different types of resonators Bagheri, Bijari & Raghebi (2015); Bindel, Quévy, Koyama, Govindjee, Demmel & Howe (2005); Darvishian, Shiari, Cho, Nagourney & Najafi (2017); Ghaffari, Ng, Ahn, Yang, Wang, Hong & Kenny (2014); Schaal, M'Closkey & Mal (2018); Sorenson & Ayazi (2014).

In addition to studies on modeling the anchor loss, many studies have investigated different methods to increase the Q of resonators by decreasing the anchor loss. It is worth pointing out that phononic crystals (PnC) are artificial materials that have their acoustic properties periodically changed in a certain structure and either hinder or allow the propagation of waves in a certain frequency range. This feature of PnCs makes them useful for reducing the anchor loss in resonators and thus, many researchers have used different 1D and 2D shaped PnCs for the anchor loss reduction Alaie, Hossein-Zadeh, Baboly, Zamani & Leseman (2016); Ardito, Cremonesi,

D'Alessandro & Frangi (2016); Bao, Bao, Lee, Bao, Khan, Zhou, Wu, Zhang & Zhang (2019); Binci, Tu, Zhu & Lee (2016); Liu, Workie, Wu, Wu, Gong, Bao & Hashimoto (2020); Wu, Bao, Zhou, Wu, Liu & Bao (2019). More recently, Workie, Wu, Bao & Hashimoto (2021) proposed different types of phononic crystals on the anchor structure, which resulted in an increase of the Q by up to 230%.

Another well-known method for increasing the Q is using wave reflectors Zhang, Luiz, Shah, Wiederhecker & Lipson (2014) which can be created by trenching the substrate layer to reduce the wave dissipation per cycle into the substrate. It is shown that acoustic in-plane reflectors were employed to increase the Q of lateral extensional MEMS resonators Harrington & Abdolvand (2011).

Despite the existing research on the use of wave reflectors for increasing the Q of MEMS resonators, there are no studies on the effect of the shape of these reflectors on their reflectivity and on its impact on resonator performance. This is a significant research gap since the anchoring structures are a major source of energy loss in resonators. Therefore, this work aims to investigate the effect of different shape trench hole arrays on the energy loss and Q of clamped-clamped beam resonators, and exploring the design parameters suited for maximum improvements in performance.

Accordingly, this work presents a study on the effect of trench hole arrays of various geometries acting as reflectors on the performance of clamped-clamped flexural beam resonators. These reflectors reduce the wave propagation from the anchors of the resonators to the substrate. A 2D model is used to simulate wave propagation in the anchoring structure of the resonators. The anchors are patterned with a series of arrayed holes of different shapes, located near the fixed ends of the resonators. Then, in order to enhance the Q of the clamped-clamped flexural beam resonators, the presented model is employed to assess various trench hole array geometries. These holes have an effect on the resonator's energy loss and can enlarge the Q, as demonstrated. The PML model is also utilized to conduct an analysis on the Q of resonators with different shapes and sizes of reflective holes on their anchors. Thereafter, the modelled resonators are

fabricated utilizing the PiezoMUMPs bulk micro-machining technology from MEMSCAP in order to experimentally validate the numerical simulations. It is found that certain hole array geometries result in an increase in Q , while the resonant frequency is varied minimally.

The design and then the fabrication process of the resonators and the structure of the reflectors are presented in Section 2.2. The numerical simulations based on 2D wave propagation and a PML model are presented in Section 2.3. This is followed by the experimental measurement of the fabricated devices in Section 2.4. Finally, a conclusion is presented.

2.2 Micro-Fabrication Process and Design

2.2.1 Fabrication using the PiezoMUMPs process

For experimental validation of the studied resonators, the PiezoMUMPS process from MEMSCAP, Crolles, France has been selected. In this fabrication process flow, depicted in Figure 2.1, a N-type silicon on insulator (SOI) wafer which is double-sided polished is used. The wafer has a 400 µm-thick substrate (handle layer) and a 10 µm-thick conductive silicon device layer due to top-side doping. A thin layer of 0.2 µm-thick thermal oxide of SiO_2 is deposited and patterned onto the wafer as the first step as an insulating layer. This layer provides the isolation of the device layer from the Al metal layer. The process is followed by the deposition of the 0.5 µm-thick piezoelectric layer which is AlN. This layer is patterned using a wet etch process. In order to form the electrical interconnect, a stack consisting of 20 nm-thick Chromium (Cr) and 1 µm-thick Aluminum (Al) is patterned using the lift-off process. The 400 µm-thick bottom silicon substrate is then patterned and etched in order to create a trench and release the mechanical resonator so that it can move. Thus, the released resonators can vibrate under the effect of an excitation signal applied to the top interconnect and the device layer that sandwich the piezoelectric film. More information on this fabrication process is given in Cowen, Hames, Glukh & Hardy (2014).

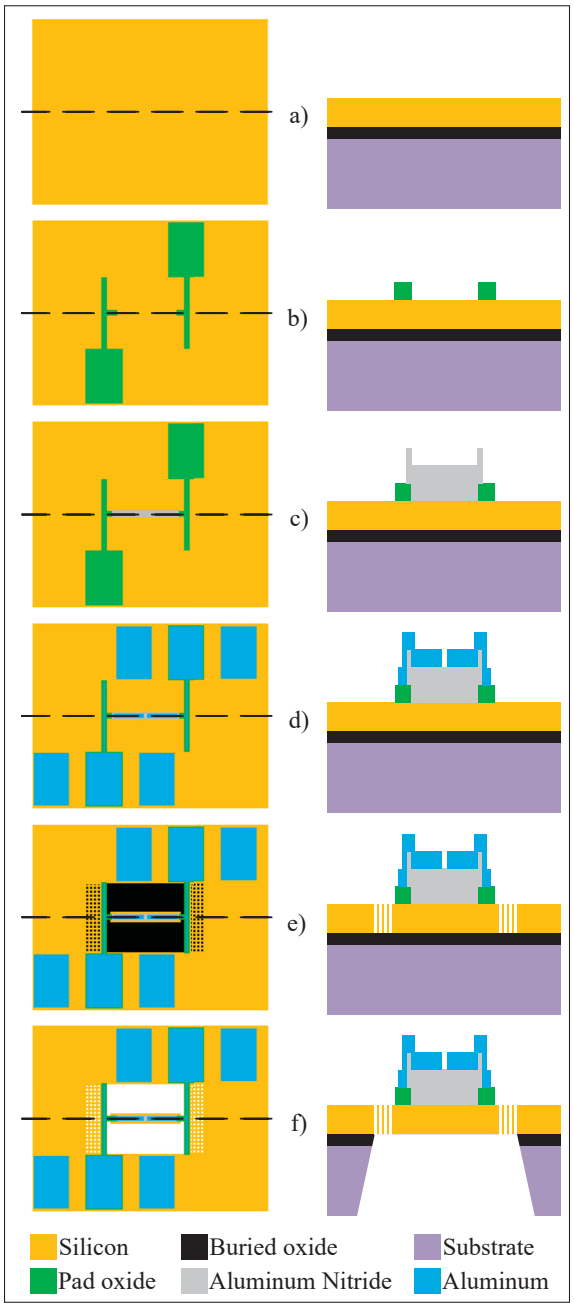

Figure 2.1 Overview of the PiezoMUMPs fabrication process used to create the clamped-clamped MEMS resonators; a) SOI wafer with 10 µm-thick top-doped device layer, b) patterning and deposition of the silicon dioxide insulating layer, c) AlN piezoelectric film deposition and patterning, d) Al layer deposition and patterning, e) device layer patterning, and f) etching of the trench

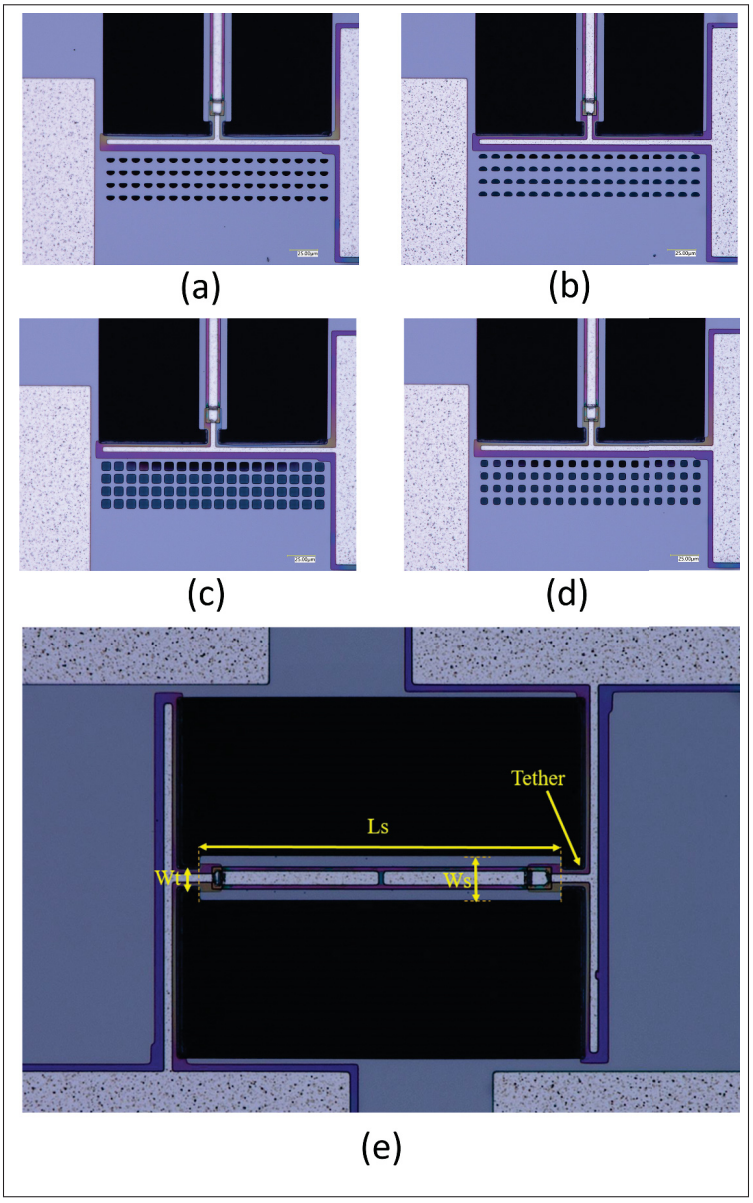

Figure 2.2 Scanning electron microscope (SEM) micrographs of the fabricated clamped-clamped beam resonators showing different trench holes on the substrate forming the arrayed-holes reflectors. Different hole geometries were fabricated long with a reference device: a) half-circle towards the resonator (named half-circle-line), b) half-circle away from the resonator (named half-circle-curve), c) large square, d) small-square, and e) reference device with no reflector

The fabricated resonators, shown in Figure 2.2, have dimensions of 225 µm in length (L_R) and 25 µm in width (W_R). The tether length on each end of the beam is 12.5 µm. Table 2.1 summarizes the device dimensions. It is worth pointing out that the energy dissipation mechanism in the resonator primarily occurs through the tether, resulting in an inversely proportional relationship between the tether width and the Q. As the width of the tether increases, the surface area exposed to the surrounding medium increases, leading to an increase in the energy loss and a decrease in the Q. Conversely, a reduction in tether width results in a decreased surface area and lower energy dissipation, thus resulting in an improvement in the Q and increased energy storage capacity. Accordingly, in order to reduce the energy loss, the width of the tether is set to be 10 µm, which is chosen based on the minimum allowed dimension by the design rules of PiezoMUMPS. This minimizes the escape of elastic waves from the resonator and decreases the Q reduction. The boundary of the trench below the resonator is set to be at the start of the reflector structure.

To create the reflectors, a set of identical holes are defined, consisting of 4 rows of 18 columns each, with a spacing of 20 µm in both x and y directions. This array of holes is placed on the substrate 20 µm apart from the cantilever tether. To investigate the effect of the reflector shape on the wave reflection and the Q of the resonators, several beam resonators were fabricated with different shapes of holes. The following shapes are considered: half-circles with a diameter of 8 µm facing toward the resonator (named half-circle-line), shown in Figure 2.2(a), similar half-circles facing away from the resonator (named half-circle-curve), shown in Figure 2.2(b), large 8 µm -wide squares (named large square), shown in Figure 2.2(c) and smaller 6 µm-wide squares (named small square) which is shown in Figure 2.2(d). A reference device consisting of a clamped-clamped resonator is also created without holes in order to compare the effects of the hole arrays on the anchor losses, shown in Figure 2.2(e).

Table 2.1 Dimensions of the resonator and reflector holes

Feature	Size (μm)
Resonator length (L_R)	200
Resonator width (W_R)	25
Tether length	12.5
Tether width	10
Piezoelectric layer width	15
Metal electrode width	7
Big square side	8
Small square side	6
Half circles diameter	8
Arrays pitch (both directions)	11

2.3 Simulation Results

2.3.1 Wave Propagation

The vibration of the flexural beam resonators generates elastic energy in the anchors of the resonator. This elastic energy travels to the substrate through the anchors and the dissipation of this energy leads to the energy loss that reduces the Q Cross & Lifshitz (2001).

According to beam theory, the displacement and velocity are assumed to be zero at the anchor locations of a clamped-clamped beam resonator. However, the vibration of the resonator generates alternating stress at this location (i.e., anchor points). This alternating force propagates into the substrate and eventually dissipates, leading to the anchor loss in the resonator. This behavior is graphically shown in Figure 2.3, where the numerically extracted resonant frequencies of the resonator with reflectors of different geometries on their anchors are also shown.

In this section, numerical analysis of the energy dissipation was carried-out using the COMSOL Multiphysics software package in the time-domain to investigate the energy dissipation behavior for the various anchoring structures. First, it is assumed that the elastic wave that travels into the substrate in the z-direction, will not reflect back to the resonator, and will be dissipated in the

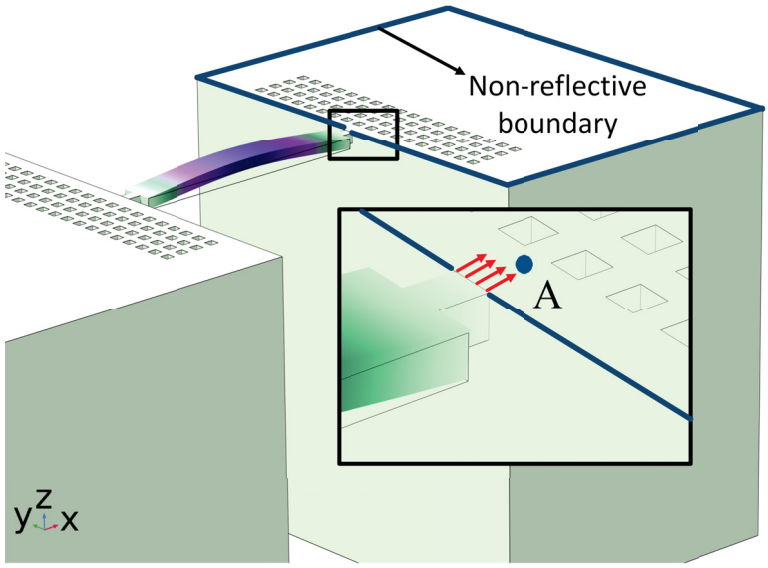

Reflector holes shape	Res. freq. (MHz)
Half circle-curve	1.029
Half circle-line	1.102
Big square	1.091
Small square	1.064
No holes	1.103

Figure 2.3 Representation of the mode shape of the resonator, placement of the reflective arrayed holes and the non-reflective boundaries. Red arrows represent the energy loss direction with the table showing the frequency of each design. Resonant frequencies are also indicated for different reflector geometries

thick substrate. It is worth mentioning that the substrate is assumed as an infinite medium in the simulation study. Furthermore, the energy that passes the reflective holes is also considered to travel to the infinite medium and be dissipated.

In order to demonstrate that the initial postulation mentioned above is valid and that the out-of-plane displacement and velocity are assumed to be zero at the anchors, the beam was electrically excited at its first resonant mode and the deformation of the anchoring point, labeled in Figure 2.3 was computed along the x-axis and z-axis. With reference to Figure 2.4, it can be seen that the out-of-plane displacement (i.e., z-axis) of point "A" on the anchor is significantly smaller than the displacement obtained along the lateral axis (i.e., x-axis). This is in agreement with our hypothesis that the out-of-plane motion and stress in the anchors are negligible comparing to the

in-plane motion and stress. Therefore, it is possible to simplify the simulation to a 2D numerical analysis and the anchor can be considered as a thin plate with a thickness of 10 µm. The stress generated by the vibration of the resonator will travel from the anchor points.

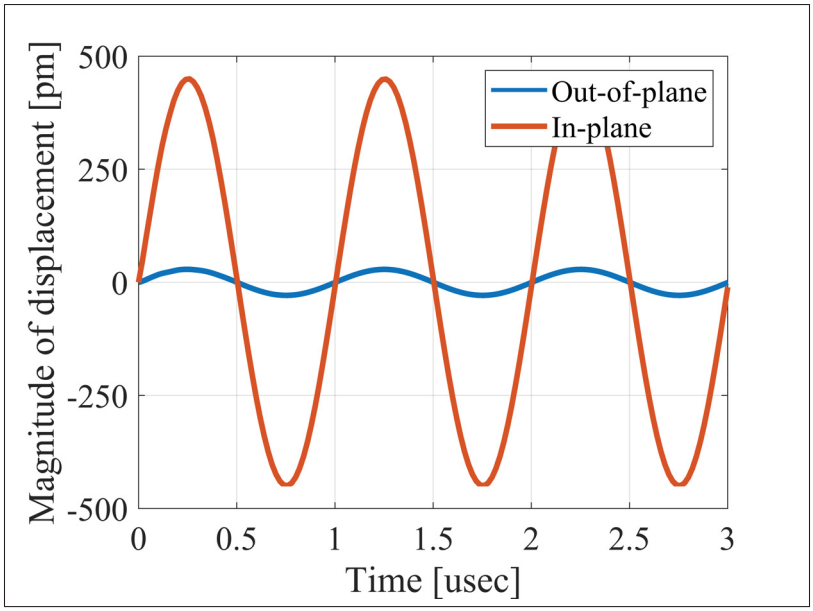

Figure 2.4 Comparison of vertical and lateral displacement at the anchor

The total amount of energy that passes the reflective holes and reaches the non-reflecting boundaries can then be indicative of the energy loss in a resonator. The energy that passes through the reflectors is considered to be dissipated, and lost into the substrate. In order to mimic this dissipation of the energy, a non-reflecting boundary is employed at the vicinity of the anchor, as shown in Figure 2.3. As such, no wave can be reflected back to the vibrating beam after passing the holes. In this finite elements method (FEM) analysis of the wave propagation in the anchors, the amount of elastic energy that passes the substrate and reaches the non-reflecting boundary represents the dissipated energy. This was observed in a 2D medium where the total energy lost in the non-reflecting boundary was quantified when the anchor point was excited by 3 periods of a sinusoidal force. The four different reflector geometries were studied with this method. It should be noted that the sinusoidal forces are exerted at the resonant frequency of each structure, as listed in Figure 2.3. The results of this computation are shown in Figure 2.5,

where in order to provide a representative comparison, the total energy losses of the resonators are normalized to the resonator with no hole in its anchoring structure.

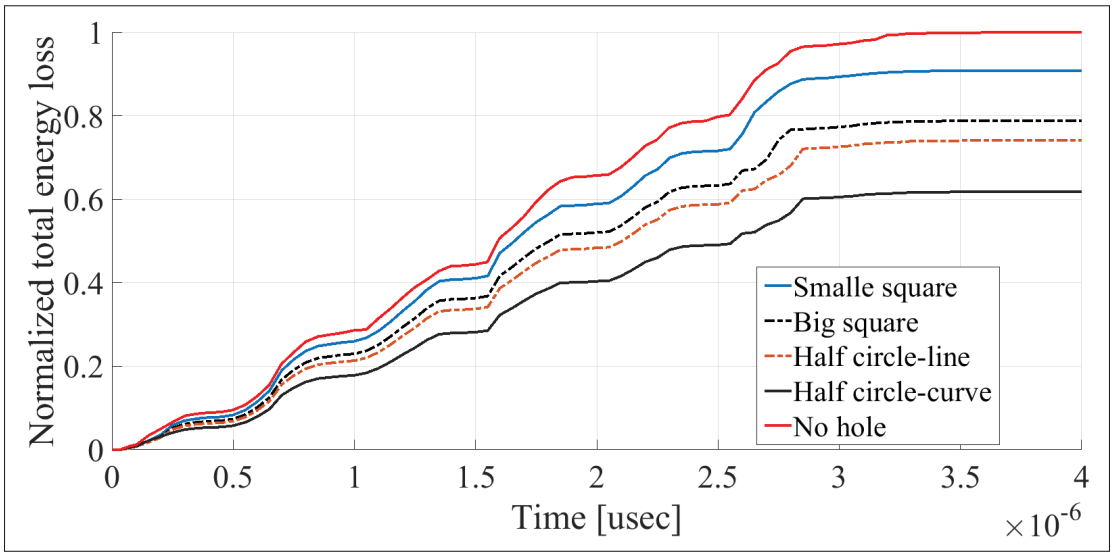

Figure 2.5 Normalized total energy transferred to the substrate over time for the different reflector geometries studied

According to Figure 2.5, the results indicate that, among the resonators evaluated, the one without a reflector had the highest overall energy loss, while the resonator with holes in the shape of half-circle-curve has the lowest energy loss. This suggests that the reflective holes impede wave dissipation and that the half-circle-curve shaped holes have the most efficient wave reflection properties.

To further demonstrate the effectiveness of the employed reflective holes for each standalone resonator, the wave propagation in the anchoring structures is graphically illustrated in Table 2.2. The data clearly demonstrates that the absence of holes on the anchoring structure of the resonator leads to a significant loss of energy as the wave travels towards the substrate without reflection and ultimately dissipates. In contrast, the presence of holes in the anchoring structure of the resonators effectively reflects the wave back towards the energy source, resulting in a lower energy loss.

Table 2.2 Visualization of the wave propagation from the anchor to the substrate at three different times

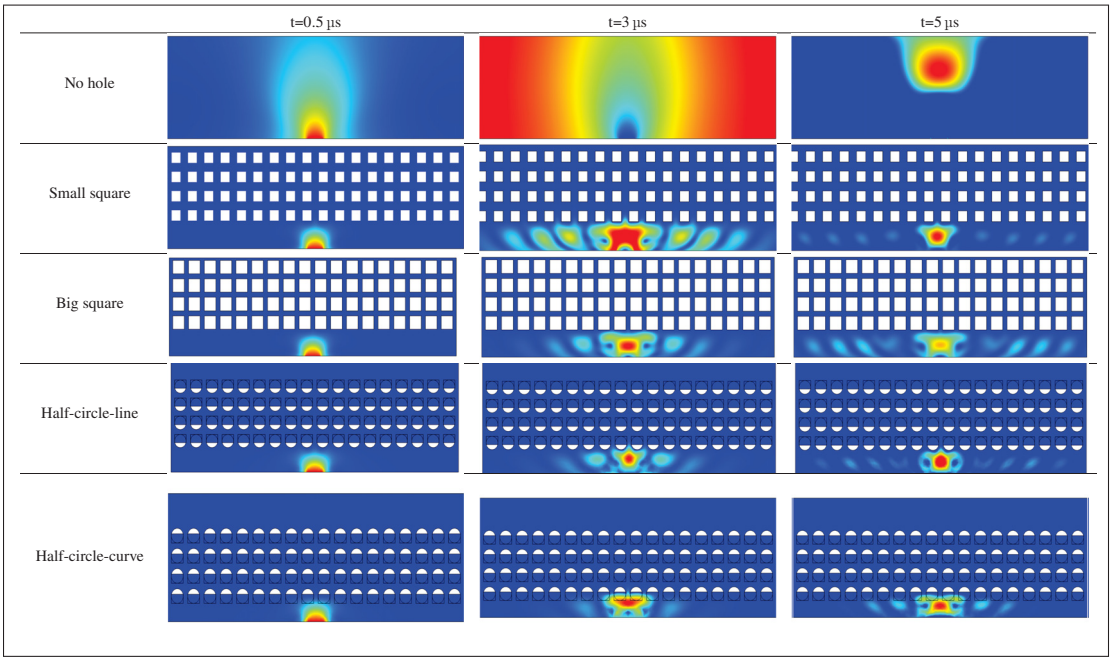

Note: The anchored edge of the beam is at the bottom of each image.

Furthermore, it can be deduced that the shape of the holes plays an important role in the effectiveness of the arrayed hole reflectors. The half-circle-curve shape, in particular, is observed to be highly effective in reflecting the energy back toward the resonator. This highlights the importance of considering the geometric properties of the reflector holes in the design of resonators to minimize energy loss.

2.3.2 Perfectly Matched Layer

This section serves to present the results of the numerical analysis of the resulting Q of the clamped-clamped resonators with the different reflectors. The perfectly matched layer (PML), which is a well-known numerical method to predict the Q of resonators was proposed by Berenger (1994) for electromagnetic wave problems. The concept of a PML is to create an artificial boundary layer around the simulation domain that absorbs the outgoing waves, mimicking the behavior of an infinite domain. The method was later expanded and re-integrated for wave-like

equations Turkel & Yefet (1998), and applied to curvilinear coordinates Collino & Monk (1998). Afterwards, the PML method was developed for complex space coordinates Teixeira & Chew (2000) and later on for anisotropic heterogeneous media Collino & Tsogka (2001) that act as an infinite domain, and eliminate the reflections of the lost waves back towards the resonator. Due to the limitations in fully modelling the substrate, researchers often rely on PML as a way to measure the anchor loss in MEMS resonators Gerrard *et al.* (2015); Park & Park (2004). This method is based on the FEM, with the PML serving as a simulated boundary layer that has the ability to absorb the energy of the acoustic waves coming from the resonating MEMS device Bindel & Govindjee (2005).

In order to assess the potential impact of reflective holes on the energy loss of the clamped-clamped resonators, we employed this method utilizing the PML option in the COMSOL Multiphysics software package. The method of stretched coordinates is employed in COMSOL to dampen the waves traveling perpendicular to the PML device interface.

Figure 2.6 shows the positioning of the resonator with symmetry on a hemispherical PML. In order to obtain the best matching results, the hemispherical PML diameter (d) is set to 10.5 mm as the PML size should be 20% greater than the wavelength in silicon at the resonance frequency, i.e., 1.1 MHz Bernstein, Bancu, Bauer, Cook, Kumar, Newton, Nyinjee, Perlin, Ricker, Teynor et al. (2015). In addition, the mesh is more finely defined in the vicinity of the resonator, notably on the anchoring structure as is shown in the figure inset. Table 2.3 presents the results of the PML analysis for different anchor types, showing that the PML predicts that placing holes on the anchors increases the Q, with varying effectiveness for each hole geometry. This is consistent with the results of the 2D wave propagation model previously discussed. In fact, the PML model predicts that the Q of the resonator with half-circle-curve geometry is the highest while the resonator with small square-shaped holes has the least improvement in its Q. As expected, all of the reflectors yield a better Q than the structure without holes.

In order to readily compare the Q extracted from the PML analysis to the measurements results later in this paper, these results are included in Table 2.4 as Q_{PML}.

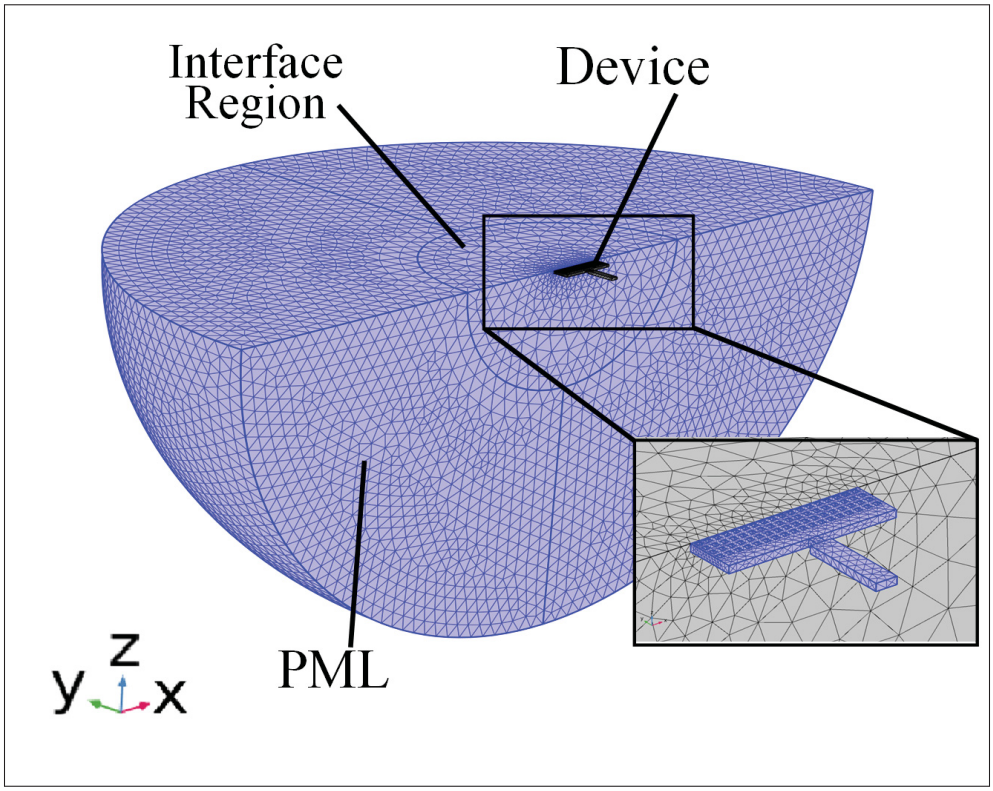

Figure 2.6 Anchor loss model implemented in COMSOL showing the resonator device, interface region and the PML area, with the fine mesh used at the resonator periphery shown in the inset

Table 2.3 Impact of hole geometry on the Q, as obtained by PML analysis

Reflector holes shape	(Q_{PML})
Half circle-curve	4590
Half circle-line	4320
Big square	4023
Small square	3735
No holes	3159

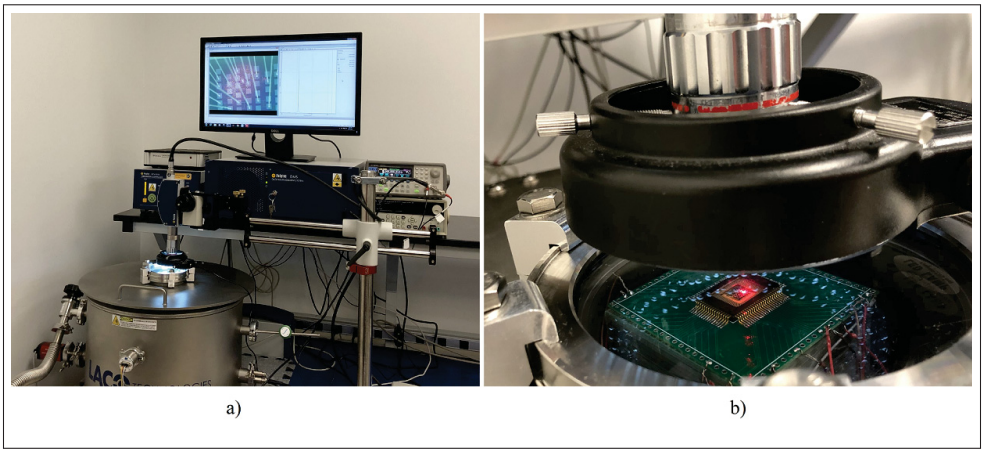

Figure 2.7 Picture of the vibrometer test bench a) wide view, b) zoomed-in view of the device in the vacuum chamber.

2.4 Experimental Results

2.4.1 Description of the Experimental Test Setup

In order to compare the results obtained from the 2D wave propagation and PML models for anchor loss, frequency response measurements were conducted on the fabricated resonators. In this study, a vibrometer (OFV-2570 Polytec controller and the Polytec laser OFV-534) was used to measure the frequency responses of the prototyped resonators. From the measured frequency responses, the mechanical Q of the resonators were calculated. Figure **??** depicts the test setup for measuring the frequency and Q of the studied MEMS resonators. The device is placed inside the vacuum chamber, which minimizes the effects of air damping on the measurements. The signal generator is connected to the device and provides the excitation signal for the resonator. The vacuum chamber is used in order to create an environment with minimal air damping to obtain accurate measurements of the frequency and Q of the resonator.

The vibrometer is able to characterize out-of-plane motion. The excitation of the device beam resonators is performed using a 33,250A Keysight function generator that is used to sweep a sinusoidal excitation frequency from 0.9 MHz to 1.2 MHz with an amplitude of 20 V peak-to-peak. The vibrometer laser is focused on the midpoint of the resonators where the

maximum displacement occurs in the first mode shape of the clamped-clamped resonators. In order to eliminate the presence of air damping in the measurements, the pressure of the chamber was reduced to 3 m.

2.4.2 Anchor stiffness

First, to validate the rigidity of the anchors and demonstrate that the anchoring structure does not experience any out-of-plane motion and that the vertical movement on the anchors is negligible, the out-of-plane displacement of the anchoring structure of the device with no holes on its anchoring structure is measured. Figure 2.8a illustrates the measured vertical displacement of points along the anchoring structure and the beam shown in Figure 2.8b. In Figure 2.8a, point zero on the x-axis denotes the anchoring point, where the tether connects the resonator to the anchoring structure. It can be observed that there is no vertical movement across the anchoring structure and that the movement amplitude increases toward the center of the beam, as expected by the first mode of resonance of the beam that is being excited. Hence, it is possible to conclude that the 2D model used in this study is appropriate.

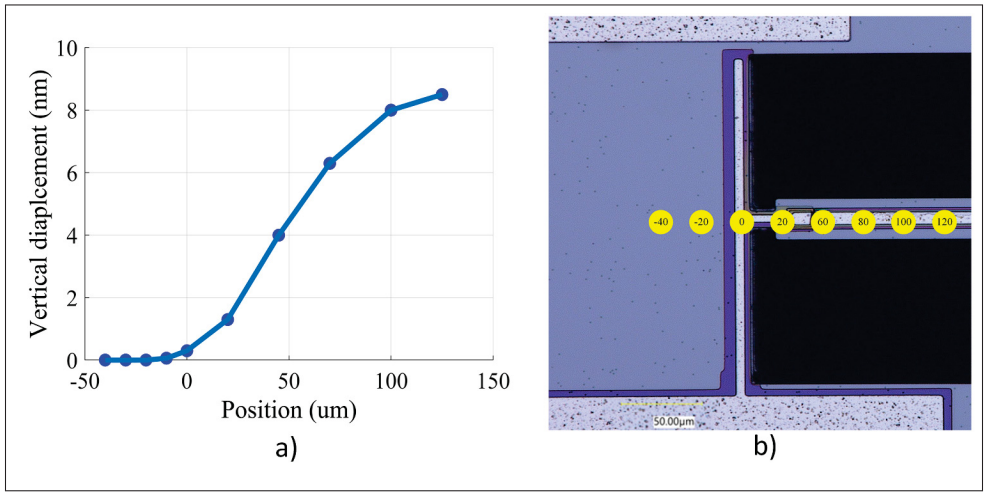

Figure 2.8 a) Vertical displacement amplitude across the resonator left half measured at the resonating frequency, and b) SEM picture of half of the clamped-clamped beam resonator with the measurement points where the vibrometer laser was focused

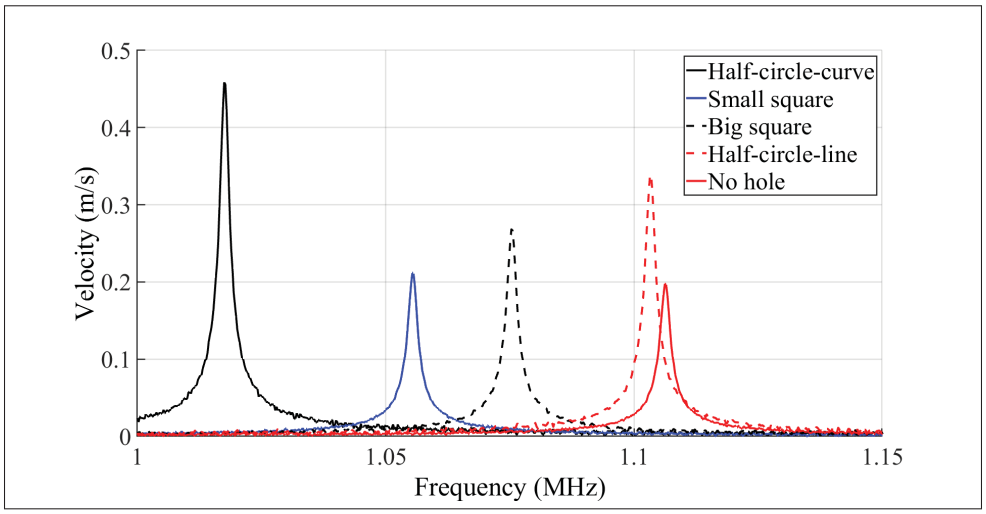

Figure 2.9 Frequency response of the velocity of the central point of the resonators in air

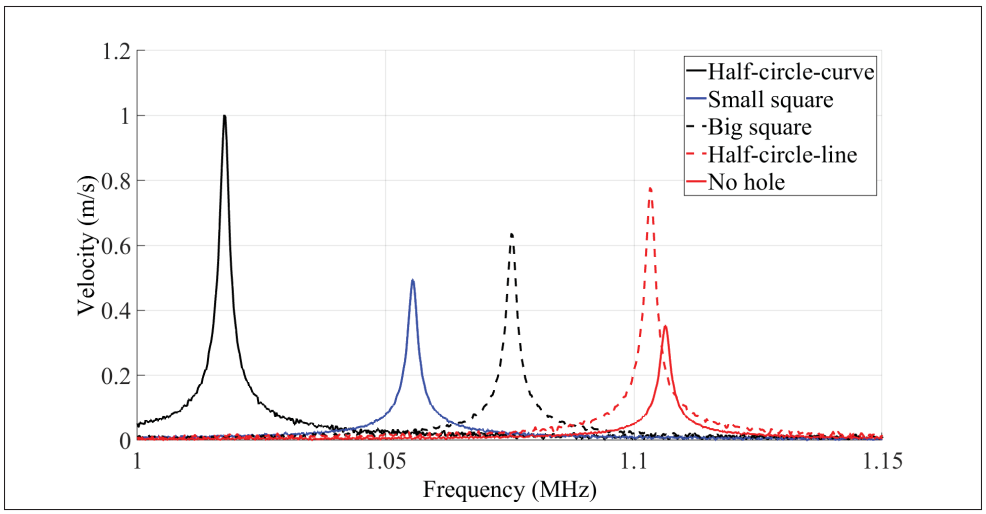

Figure 2.10 Frequency response of the velocity of the central point of the resonators in vacuum

2.4.3 Frequency response

Figure 2.9 and Figure 2.10 respectively illustrate the frequency response of the resonator velocity in air and vacuum. The results are shown for each of the five different MEMS beam resonators,

Table 2.4 Impact of the reflector hole geometry on the Q of the resonators

	Hole type	Half circle-curve	Half circle-line	Big square	Small square	No holes
Simulation	Res. freq. (MHz)	1.029	1.102	1.091	1.064	1.103
	Q_{PML}	4,590	4,320	4,023	3,735	3,159
Measurements in air	Res. freq. (MHz)	1.021±0.0022	1.042±0.0015	1.078±0.0027	1.085±0.0021	1.101±0.0023
	Q_{air}	1,620±24	1,480±21	1,340±24	1,240±19	940±21
	QR_{air}	1.70	1.57	1.42	1.31	1
Measurements in vacuum	Res. freq. (MHz)	1.024±0.0022	1.048±0.0015	1.082±0.0023	1.092±0.0018	1.108±0.0025
	Q_{vacuum}	3,630±31	3,450±44	3,100±51	2,800±39	2,100±46
	QR_{vacuum}	1.72	1.64	1.47	1.33	1

denoted according to their reflector geometry type as half-circle-curve, half-circle-line, small square, big square, and no hole.

The Q is derived from the frequency response of a resonator in both air and vacuum using the ratio of the resonant frequency f to the bandwidth Δf at 70.7% of the maximum displacement of the frequency response curve.

The results of the measured Q in both air and vacuum are listed in Table 2.4, along with the simulation results from the PML Q analysis and the resonant frequency modal analysis. In order to ensure the validity and accuracy of the test results, and minimize the impact of fabrication process variations, the testing procedure for each standalone resonator was repeated on a total of five distinct dies. Subsequently, statistical analysis was performed to calculate the average and standard deviation of the measured Qs and resonant frequencies. The relatively small deviations listed in Table 2.4 serve as evidence of the relatively good repeatability of our measurements, with minimal impact from fabrication process variation. These small deviations also ensure that the conclusions drawn are accurate.

The results show that the incorporation of reflectors on the anchoring structure of the flexural clamped-clamped beam resonators leads to an increase of the Q. It is seen that the device with half circle-curve shape holes yields the highest Q. This behavior was foreseen in Figure 2.5, as the total energy loss of the half-circle-curve device is the lowest.

The frequency response of the resonators shows that the resonance peaks of the resonators with different anchor types vary between 1.024 MHz and 1.108 MHz in vacuum and between1.021 MHz

and 1.101 MHz in air. It can be further seen that each resonator has a unique resonance frequency and amplitude of displacement. These frequency shifts are in part due to the anchoring structure type, as seen in the simulations previously presented, and can also be caused by slight geometry variations between the beams tested due to fabrication variability.

In order to provide a more representative comparison of the performance of the resonators that have reflective holes on their anchors with the performance the reference resonator that has no holes on its anchors, the Q ratio is defined as:

$$QR = \frac{Q_{device}}{Q_{Noholes}} \tag{2.3}$$

The QR is reported for the the results of the Q in both air and vacuum in Table 2.4, denoted as QR_{air} and QR_{vacuum}, respectively.

The results clearly indicate that the incorporation of reflectors can play a crucial role in enhancing the (Q) of resonators, and that the hole geometry can have a significant impact. For instance in Table 2.4, the geometry of the holes yielded a QR going from 1.33 to 1.72 in vacuum when comparing the small square holes to the better performing half-circle-curve holes. This is a significant impact as the percentage increase in Q) is more than doubled when using half-circle-curve holes instead of small square holes.

It is worthwhile to note that both the PML and measurements support the results of the 2D low-reflecting boundary method, indicating that the method is effective when the elastic wave traveling toward the thickness of the resonator is negligible. Additionally, according to the ideal beam theory, the movement and slope of displacement are assumed to be zero at the endpoints of the resonators. This assumption is supported by both the measurements and the FEM model used in this study.

Both the PML and measurements support the results of the low-reflecting boundary method, indicating that the method is effective when the elastic wave traveling toward the thickness of the resonator is negligible. Table 2.4 summarizes the results of this study using the FEM method.

The PML model only predicts variations in the Q, but it does not provide insight into the cause of these changes. Since determining the cause of changes in the Q is crucial in this study, a 2D wave propagation model was implemented. This model revealed that the presence of trenched holes in the vicinity of the anchoring points leads to the reflection of energy back towards the resonator with different degrees of effectiveness, depending on hole geometry.

2.5 Conclusion

In this study, the impact of anchoring structures on wave propagation in MEMS clamped-clamped beam flexural mode resonators was investigated with the goal of reducing anchor loss and increasing the Q. In this context, a group of clamped-clamped MEMS beam resonators, with arrays of holes of different shapes were placed on their anchoring structures to act as reflectors, and the results were compared with a reference device without holes on its anchors. The PML method was utilized to investigate the Q of the resonators with differently shaped holes. The use of the PML model to predict the Q for resonators with different shapes of holes indicated improvement of the Q with the reflectors. Notably, the half-circle-curve shaped holes was shown to lead to the highest improvement in the Q.

Furthermore, to achieve a deeper understanding of the mechanism behind this enhancement, a 2D numerical model was proposed. In this model, the anchor edges were considered as low-reflective boundaries and the sum of energy loss was calculated at these boundaries. This allowed the study of the effectiveness of the different hole geometries in preventing waves from dissipating to the substrate. The model indicated that the half-circle-curve holes caused the lowest energy escape from the anchoring structure, in agreement with the PML analysis.

The PiezoMUMPS process is used to fabricate the resonators and they were characterized. The measurements corroborated the simulations, with a significant improvement in Q observed. The highest QR was attained using the half-circle-curve hole geometry, showing an improvement in the Q by 1.7 fold in air and 1.72 fold in vacuum.

The proposed wave propagation model and the findings of this study have the potential to impact the design and optimization of resonators in a wide range of fields and applications pertaining to MEMS resonators. Notably, this work shed light into the impact of the reflector hole geometry on the Q and provided a 2D numerical model in addition to the more conventional PML method. Future work will focus on optimizing the dimensions of the reflective holes to further increase the performance of the resonators. Notably, this study could be replicated for other resonator geometries.

Acknowledgement

The authors extend their gratitude to the Natural Sciences and Engineering Research Council of Canada (NSERC) for their financial support. They also extend their appreciation to CMC Microsystems for their support in providing layout design tools and facilitating device fabrication.

Author Contributions

M.K. designed the devices, performed the experimental testing, and wrote the manuscript. M.G. and M.K designed the experimental test setup. M.K wrote the manuscript. M.G and S.N helped in improving the manuscript and F.N. supervised the work and provided expertise. All authors contributed to the writing of the paper.

CONCLUSION AND RECOMMENDATIONS

Research Summary

The primary objective of this thesis was to design and characterize bulk micromachined MEMS resonators to mitigate anchor loss and enhance the quality factor (Q). The study also aimed to investigate the tunability of flexural beam resonators. The research began by analyzing the influence of trench hole arrays with various geometries on the performance of clamped-clamped flexural beam resonators, which function as reflectors to minimize wave propagation from the anchors of the resonators to the substrate.

To achieve this, a 2D simulation model was developed to assess wave propagation within the anchoring structure of the resonators. The resonator anchors were patterned with a series of arrayed holes of different shapes, placed in proximity to the fixed ends of the resonators. A simulation model was used to evaluate a range of trench hole array geometries to optimize the quality factor (Q) of the clamped-clamped flexural beam resonators. It was demonstrated that these holes impact the energy loss of the resonator and have the potential to enhance the Q.

To further evaluate the quality factor Q of resonators with different shapes and sizes of reflective holes on their anchors, a perfectly matched layer (PML) model was employed. To experimentally validate the numerical simulations, resonators were fabricated using the PiezoMUMPs bulk micro-machining technology from MEMSCAP. The experimental results suggested that certain hole array geometries can increase the quality factor Q value of the resonator, while the resonant frequency remained relatively stable.

Secondly, a novel method for tuning the resonant frequency of beam resonators utilizing electrostatic actuators was presented. The proposed method was based on strategically placing electrostatic actuators in close proximity to the ends of the resonator, which increased the stiffness of the anchoring ends. The electrostatic actuators were operated using a DC actuation voltage

and could enter into contact with the anchors of the resonator, thereby modifying their stiffness and ultimately altering the resonance frequency of the resonator. The fabricated resonator operated in three distinct states, namely released actuators, single-side catch, and double-sided catch, yielding a significant frequency shift capability. In order to investigate the impact of these three states on the first three resonance frequencies of the resonator, a detailed numerical and experimental analysis was conducted. The study involved examination and quantification of the effect of these states on the performance of the resonator. The proposed method has the potential to be applied to a wide range of high-performance beam resonators, including MEMS sensors and communication systems.

The outcomes of this investigation have practical implications for the design and optimization of beam resonators. The results can guide the development of high-performance resonators with improved performance characteristics and better agility, which can ultimately lead to a wider spread applicability and to new applications.

Future Works and Recommendations

The presented research can still be improved in many ways. This thesis was focused on the flexural mode beam resonators and increasing their Q and tuning their frequency. However, the breath of these works can be improved using the following suggestions:

- **Applying the reflectors to other resonance modes:**

  The proposed technique has the potential to find application in a broader range of resonator modes and configurations beyond the specific beam resonator design investigated in this study. For example, the implementation of trench hole arrays, similar to those studied herein, could be utilized to enhance the quality factor of alternative resonator structures such as bulk acoustic wave resonators (e.g., Lame mode resonators and contour mode resonators). The

ability to apply this approach across diverse resonator designs underscores the versatility and general applicability of this methodology.

- **Using the proposed DC actuators for temperature compensation:**

  The tunability of a resonator can be used as compensation for the frequency drift of a resonator that is caused by the temperature increase. DC actuators can definitely be an alternative to preheating resonators using embedded heaters which is a highly power-consuming method. One such method involves the use of DC actuators to finely tune the resonator frequency, which is an attractive alternative to preheating resonators using embedded heaters that consume significant amounts of power.

  To further improve the effectiveness of this method, we recommend a modified design in which the gap between the shuttles and the anchoring beams is closed, enabling analog tuning of the frequency using a compressive force that can be generated by further activating the actuators beyond the contact is reached. This method allows for the reduction of the compressive force as the temperature rises, which leads to an increase in the resonator frequency and effectively compensates for the decrement in resonant frequency induced by temperature changes.

  This proposed approach holds significant potential for enhancing the performance of resonators in various applications, including MEMS sensors and communication systems. By addressing the issue of frequency drift caused by temperature changes, this method can improve the accuracy and reliability of resonator-based systems, leading to significant advancements in the field.

- **Using the proposed DC actuators to shift the frequency through changing the effective length of the resonator:**

One of the other factors that affect the frequency of a beam is its is its length. Therefore, manipulating the effective length of the resonator is a promising method to tune its frequency and potentially enable the realization of resonators with multiple frequencies. The electrostatic actuator approach proposed in this study can be effectively applied to beam resonator structures, allowing the extraction of distinct resonant frequencies from a single resonator, which is a crucial aspect in the design of bandpass filters for communication systems. The potential of this method to enable compact, multi-frequency resonator designs has significant implications for the development of high-performance communication and sensing technologies.

Academic Contributions

This master's study resulted in the submission of two journal papers as listed below:

- "Anchor Loss Reduction in MEMS Flexural Beam Resonators Using Trench Hole Array Reflectors" by M. Kazemi, S.Nabavi, M. Gratuze, and F.Nabki, submitted to the MDPI Micromachines, on 2023/08/18.
- "Frequency Selection in a MEMS Flexural Beam Resonator by Electrostatic Actuation" by M. Kazemi, S.Nabavi, M. Gratuze, and F.Nabki, submitted to the IEEE Journal of Microelectromechanical Systems (JMEMS), on 2023/05/17.

Academic Awards

- Awarded with "Exemption des Frais Majorés à la Maîtrise" for three consecutive semesters.
- Awarded with "ReSMiQ Scholarship Supplement for M.Sc. students" for two academic years.

LIST OF REFERENCES

Abdolvand, R., Bahreyni, B., Lee, J. E.-Y. & Nabki, F. (2016). Micromachined resonators: A review. *Micromachines*, 7(9), 160.

Agarwal, M., Park, K. K., Candler, R. N., Kim, B., Hopcroft, M. A., Chandorkar, S. A., Jha, C. M., Melamud, R., Kenny, T. W. & Murmann, B. (2006). Nonlinear characterization of electrostatic MEMS resonators. *2006 IEEE International Frequency Control Symposium and Exposition*, pp. 209–212.

Alaie, S., Hossein-Zadeh, M., Baboly, M. G., Zamani, M. & Leseman, Z. C. (2016). Enhancing mechanical quality factors of micro-toroidal optomechanical resonators using phononic crystals. *Journal of Microelectromechanical Systems*, 25(2), 311–319.

Alcheikh, N., Ramini, A., Hafiz, M. A. A. & Younis, M. I. (2017). Tunable clamped–guided arch resonators using electrostatically induced axial loads. *Micromachines*, 8(1), 14.

Alcheikh, N., Kosuru, L., Kazmi, S. N. R. & Younis, M. I. (2020). In-plane air damping of micro- and nano-mechanical resonators. *Journal of Micromechanics and Microengineering*, 30(3), 035007.

Alsaleem, F. M. & Younis, M. I. (2010). Stabilization of electrostatic MEMS resonators using a delayed feedback controller. *Smart Materials and Structures*, 19(3), 035016.

Aoust, G., Levy, R., Bourgeteau, B. & Le Traon, O. (2015). Viscous damping on flexural mechanical resonators. *Sensors and Actuators A: Physical*, 230, 126–135.

Ardito, R., Cremonesi, M., D'Alessandro, L. & Frangi, A. (2016). Application of optimally-shaped phononic crystals to reduce anchor losses of MEMS resonators. *2016 IEEE International Ultrasonics Symposium (IUS)*, pp. 1–3.

Azizi, S., Ghazavi, M. R., Rezazadeh, G., Ahmadian, I. & Cetinkaya, C. (2014). Tuning the primary resonances of a micro resonator, using piezoelectric actuation. *Nonlinear dynamics*, 76, 839–852.

Bagheri, M., Bijari, A. & Raghebi, M. (2015). Modeling and calculating the anchor loss quality factor in the plunging-mode vibrations of a micromechanical rectangular-plate resonator with two T-shaped support beams. *Modares Mechanical Engineering*, 14(12), 75–84.

Bajpai, R. & Zaghloul, M. (2009). Modeling a fixed-fixed beam nano biosensor using equivalent electrical circuit technique. *2009 IEEE/NIH Life Science Systems and Applications Workshop*, pp. 58–61.

Banerji, S., Fernandez, D. & Madrenas, J. (2017). Characterization of CMOS-MEMS resonant pressure sensors. *IEEE Sensors Journal*, 17(20), 6653–6661.

Bao, F.-H., Bao, J.-F., Lee, J. E.-Y., Bao, L.-L., Khan, M. A., Zhou, X., Wu, Q.-D., Zhang, T. & Zhang, X.-S. (2019). Quality factor improvement of piezoelectric MEMS resonator by the conjunction of frame structure and phononic crystals. *Sensors and Actuators A: Physical*, 297, 111541.

Basirico, L. & Lanzara, G. (2012). Moving towards high-power, high-frequency and low-resistance CNT supercapacitors by tuning the CNT length, axial deformation and contact resistance. *Nanotechnology*, 23(30), 305401.

Basu, J. & Bhattacharyya, T. K. (2011). Microelectromechanical resonators for radio frequency communication applications. *Microsystem technologies*, 17(10), 1557–1580.

Baù, M., Ferrari, M., Ferrari, V., Ali, A. & Lee, J.-Y. (2019). Automatic Compensation of Parallel Capacitance of TPoS MEMS Resonator for Accurate Frequency Tracking with PLL-Based Oscillator Circuit. pp. 273–278.

Bell, D. J., Lu, T., Fleck, N. A. & Spearing, S. M. (2005). MEMS actuators and sensors: observations on their performance and selection for purpose. *Journal of micromechanics and microengineering*, 15(7), S153.

Berenger, J.-P. (1994). *A Perfectly Matched Layer for the Absorption of Electromagnetic Waves*.

Bernstein, J. J., Bancu, M. G., Bauer, J. M., Cook, E. H., Kumar, P., Newton, E., Nyinjee, T., Perlin, G. E., Ricker, J. A., Teynor, W. A. et al. (2015). High Q diamond hemispherical resonators: fabrication and energy loss mechanisms. *Journal of Micromechanics and Microengineering*, 25(8), 085006.

Bian, X., Jin, H., Wang, X., Dong, S., Chen, G., Luo, J., Deen, M. J. & Qi, B. (2015). UV sensing using film bulk acoustic resonators based on Au/n-ZnO/piezoelectric-ZnO/Al structure. *Scientific reports*, 5(1), 1–5.

Binci, L., Tu, C., Zhu, H. & Lee, J.-Y. (2016). Planar ring-shaped phononic crystal anchoring boundaries for enhancing the quality factor of Lamb mode resonators. *Applied Physics Letters*, 109(20), 203501.

Bindel, D. S. & Govindjee, S. (2005). Elastic PMLs for resonator anchor loss simulation. *International Journal for Numerical Methods in Engineering*, 64(6), 789–818.

Bindel, D. S., Quévy, E., Koyama, T., Govindjee, S., Demmel, J. W. & Howe, R. T. (2005). Anchor loss simulation in resonators. *Proceedings of the IEEE International Conference on Micro Electro Mechanical Systems (MEMS)*, pp. 133–136. doi: 10.1109/memsys.2005.1453885.

Blue, R., Brown, J. G., Li, L., Bauer, R. & Uttamchandani, D. (2020). MEMS gas flow sensor based on thermally induced cantilever resonance frequency shift. *IEEE Sensors Journal*, 20(8), 4139–4146.

Bruckner, K., Cimalla, V., Niebelschutz, F., Stephan, R., Tonisch, K., Ambacher, O. & Hein, M. (2007). Gas pressure sensing based on MEMS resonators. *SENSORS, 2007 IEEE*, pp. 1251–1254.

Bustillo, J. M., Howe, R. T. & Muller, R. S. (1998). Surface micromachining for microelectromechanical systems. *Proceedings of the IEEE*, 86(8), 1552–1574.

Cai, C., Tan, J., Hua, D., Qin, M. & Zhu, N. (2018). Piezoresistive temperature sensors fabricated by a surface micromachining CMOS MEMS process. *Scientific Reports*, 8(1), 17065.

Campanella, H., Narducci, M., Merugu, S. & Singh, N. (2017). Dual MEMS resonator structure for temperature sensor applications. *IEEE Transactions on Electron Devices*, 64(8), 3368–3376.

Candler, R. N., Duwel, A., Varghese, M., Chandorkar, S. A., Hopcroft, M. A., Park, W.-T., Kim, B., Yama, G., Partridge, A., Lutz, M. et al. (2006). Impact of geometry on thermoelastic dissipation in micromechanical resonant beams. *Journal of Microelectromechanical Systems*, 15(4), 927–934.

Cao, Y. & Sepúlveda, N. (2019). Interface stress for bidirectional frequency tuning of Prebuckled vanadium dioxide MEMS resonators. *Advanced Materials Interfaces*, 6(21), 1900887.

Cassella, C. & Piazza, G. (2016). Thick aluminum nitride contour-mode resonators mitigate thermoelastic damping. *2016 IEEE International Frequency Control Symposium (IFCS)*, pp. 1–2.

Chandorkar, S., Agarwal, M., Melamud, R., Candler, R., Goodson, K. & Kenny, T. (2008). Limits of quality factor in bulk-mode micromechanical resonators. *2008 IEEE 21st international conference on micro electro mechanical systems*, pp. 74–77.

Chang, Y., Wei, J. & Lee, C. (2020). Metamaterials–from fundamentals and MEMS tuning mechanisms to applications. *Nanophotonics*, 9(10), 3049–3070.

Chauhan, S. S., Joglekar, M. M. & Manhas, S. K. (2019). High power density CMOS compatible micro-machined MEMs energy harvester. *IEEE Sensors Journal*, 19(20), 9122–9130.

Chellasivalingam, M., Graves, B., Boies, A. & Seshia, A. A. (2020). Mass tuning in weakly coupled low-Q piezoelectric MEMS resonator arrays for particulate sensing. *2020 IEEE 33rd International Conference on Micro Electro Mechanical Systems (MEMS)*, pp. 761–764.

Chimeh, H. E., Nabavi, S., Al Janaideh, M. & Zhang, L. (2021). Deep-learning-based optimization for a low-frequency piezoelectric MEMS energy harvester. *IEEE Sensors Journal*, 21(19), 21330–21341.

Chuang, W.-C., Lee, H.-L., Chang, P.-Z. & Hu, Y.-C. (2010). Review on the modeling of electrostatic MEMS. *Sensors*, 10(6), 6149–6171.

Collino, F. & Monk, P. (1998). The perfectly matched layer in curvilinear coordinates. *SIAM Journal on Scientific Computing*, 19(6), 2061–2090.

Collino, F. & Tsogka, C. (2001). Application of the perfectly matched absorbing layer model to the linear elastodynamic problem in anisotropic heterogeneous media. *Geophysics*, 66(1), 294–307.

Conway, N. J., Traina, Z. J. & Kim, S.-G. (2007). A strain amplifying piezoelectric MEMS actuator. *Journal of Micromechanics and Microengineering*, 17(4), 781.

Cowen, A., Hames, G., Glukh, K. & Hardy, B. (2014). PiezoMUMPs design handbook. *MEMSCAP Inc*, 1.

Cross, M. & Lifshitz, R. (2001). Elastic wave transmission at an abrupt junction in a thin plate with application to heat transport and vibrations in mesoscopic systems. *Physical Review B*, 64(8), 085324.

Darvishian, A., Shiari, B., Cho, J. Y., Nagourney, T. & Najafi, K. (2017). Anchor loss in hemispherical shell resonators. *Journal of Microelectromechanical Systems*, 26(1), 51–66.

Davis, Z. J., Svendsen, W. & Boisen, A. (2007). Design, fabrication and testing of a novel MEMS resonator for mass sensing applications. *Microelectronic Engineering*, 84(5-8), 1601–1605.

Dennis, J. O., Ahmed, A. Y., Khir, M. M. & Rabih, A. A. S. (2015). Modelling and Simulation of the Effect of Air Damping on the Frequency and Quality factor of a CMOS-MEMS Resonator. *Appl. Math. Infor. Sci.(AMIS)*, 9, 729–737.

Deshpande, P. P., Pande, R. S. & Patrikar, R. M. (2020). Fabrication and characterization of zinc oxide piezoelectric MEMS resonator. *Microsystem Technologies*, 26(2), 415–423.

Développement, Y. Status of the MEMS Industry 2020: Market and Technology Report (Sample), jun 2020. *URL: https://s3. i-micronews. com/uploads/2020/07/YDR20104-Status-of-the-MEMS-Industry-2020-Sample-Yole-Développement. pdf*.

DeVoe, D. L. (2001). Piezoelectric thin film micromechanical beam resonators. *Sensors and Actuators A: Physical*, 88(3), 263–272.

Dubuc, D., Grenier, K. & Iannacci, J. (2018). RF-MEMS for smart communication systems and future 5G applications. In *Smart Sensors and MEMS* (pp. 499–539). Elsevier.

Duwel, A., Candler, R. N., Kenny, T. W. & Varghese, M. (2006). Engineering MEMS resonators with low thermoelastic damping. *Journal of microelectromechanical systems*, 15(6), 1437–1445.

Eidi, A. (2022). An Ultra-Low Frequency and Low-Pressure Capacitive Blood Pressure Sensor Based on Micro-Mechanical Resonator. *Sensing and Imaging*, 23(1), 1–12.

Fadel, L., Dufour, I., Lochon, F. & Francais, O. (2004). Signal-to-noise ratio of resonant microcantilever type chemical sensors as a function of resonant frequency and quality factor. *Sensors and Actuators B: Chemical*, 102(1), 73–77.

Gerrard, D. D., Ng, E. J., Ahn, C. H., Hong, V. A., Yang, Y. & Kenny, T. W. (2015). Modeling the effect of anchor geometry on the quality factor of bulk mode resonators. *2015 Transducers-2015 18th International Conference on Solid-State Sensors, Actuators and Microsystems (TRANSDUCERS)*, pp. 1997–2000.

Ghaffari, S., Ng, E. J., Ahn, C. H., Yang, Y., Wang, S., Hong, V. A. & Kenny, T. W. (2014). Accurate modeling of quality factor behavior of complex silicon MEMS resonators. *Journal of Microelectromechanical Systems*, 24(2), 276–288.

Göktaş, H. & Zaghloul, M. E. (2014). Tuning in-plane fixed-fixed beam resonators with embedded heater in CMOS technology. *IEEE Electron Device Letters*, 36(2), 189–191.

Gong, S. & Piazza, G. (2012). Design and analysis of lithium–niobate-based high electromechanical coupling RF-MEMS resonators for wideband filtering. *IEEE Transactions on Microwave Theory and Techniques*, 61(1), 403–414.

Gusso, A. (2020). Nonlinear damping in suspended beam micro-and nanoresonators due to surface loss. *Journal of Sound and Vibration*, 467, 115067.

Guzman, P., Dinh, T., Phan, H.-P., Joy, A. P., Qamar, A., Bahreyni, B., Zhu, Y., Rais-Zadeh, M., Li, H., Nguyen, N.-T. et al. (2020). Highly-doped SiC resonator with ultra-large tuning frequency range by Joule heating effect. *Materials & Design*, 194, 108922.

Hajjaj, A. Z., Hafiz, M. A. & Younis, M. I. (2017a). Mode coupling and nonlinear resonances of MEMS arch resonators for bandpass filters. *Scientific reports*, 7(1), 1–7.

Hajjaj, A. Z., Ramini, A., Alcheikh, N. & Younis, M. I. (2017b). Electrothermally tunable arch resonator. *Journal of Microelectromechanical Systems*, 26(4), 837–845.

Hajjam, A., Logan, A., Pandiyan, J. & Pourkamali, S. (2011). High frequency thermal-piezoresistive MEMS resonators for detection of organic gases. *2011 Joint Conference of the IEEE International Frequency Control and the European Frequency and Time Forum (FCS) Proceedings*, pp. 1–5.

Hao, Z., Erbil, A. & Ayazi, F. (2003). An analytical model for support loss in micromachined beam resonators with in-plane flexural vibrations. *Sensors and Actuators A: Physical*, 109(1-2), 156–164. doi: 10.1016/J.SNA.2003.09.037.

Harrington, B. & Abdolvand, R. (2011). In-plane acoustic reflectors for reducing effective anchor loss in lateral–extensional MEMS resonators. *Journal of Micromechanics and Microengineering*, 21(8), 085021.

He, Q., Liu, J., Yang, B., Wang, X., Chen, X. & Yang, C. (2014). MEMS-based ultrasonic transducer as the receiver for wireless power supply of the implantable microdevices. *Sensors and Actuators A: Physical*, 219, 65–72.

He, R., Feng, X., Roukes, M. & Yang, P. (2008). Self-transducing silicon nanowire electromechanical systems at room temperature. *Nano letters*, 8(6), 1756–1761.

Herrera-May, A. L., Soler-Balcazar, J. C., Vázquez-Leal, H., Martínez-Castillo, J., Vigueras-Zuñiga, M. O. & Aguilera-Cortés, L. A. (2016). Recent advances of MEMS resonators for Lorentz force based magnetic field sensors: design, applications and challenges. *Sensors*, 16(9), 1359.

Hersee, S. & Duchemin, J. (1982). Low-pressure chemical vapor deposition. *Annual Review of Materials Science*, 12(1), 65–80.

Hsu, W.-T. (2007). Low cost packages for MEMS oscillators. *2007 32nd IEEE/CPMT International Electronic Manufacturing Technology Symposium*, pp. 273–277.

Hsu, W.-T. & Pai, M. (2007). The new heart beat of electronics-silicon MEMS oscillators. *2007 Proceedings 57th Electronic Components and Technology Conference*, pp. 1895–1899.

Hung, L.-W. & Nguyen, C. T.-C. (2011). Capacitive-piezoelectric AlN resonators with Q> 12,000. *2011 IEEE 24th International Conference on Micro Electro Mechanical Systems*, pp. 173–176.

Ibrahim, S. W. & Ali, W. G. (2012). A review on frequency tuning methods for piezoelectric energy harvesting systems. *Journal of renewable and sustainable energy*, 4(6), 062703.

Jaber, N., Ilyas, S., Shekhah, O., Eddaoudi, M. & Younis, M. I. (2018). Multimode MEMS resonator for simultaneous sensing of vapor concentration and temperature. *IEEE Sensors Journal*, 18(24), 10145–10153.

Jha, A. R. (2008). *MEMS and nanotechnology-based sensors and devices for communications, medical and aerospace applications*. CRC Press.

Jha, C., Bahl, G., Melamud, R., Chandorkar, S., Hopcroft, M., Kim, B., Agarwal, M., Salvia, J., Mehta, H. & Kenny, T. (2007). CMOS-compatible dual-resonator MEMS temperature sensor with milli-degree accuracy. *TRANSDUCERS 2007-2007 International Solid-State Sensors, Actuators and Microsystems Conference*, pp. 229–232.

Jmai, B., Gahgouh, S. & Gharsallah, A. (2017). A novel reconfigurable MMIC antenna with RF-MEMS resonator for radar application at K and Ka bands. *International Journal of Advanced Computer Science and Applications*, 8(5).

Kaajakari, V., Mattila, T., Lipsanen, A. & Oja, A. (2005). Nonlinear mechanical effects in silicon longitudinal mode beam resonators. *Sensors and Actuators A: Physical*, 120(1), 64–70.

Karabalin, R., Matheny, M., Feng, X., Defaÿ, E., Le Rhun, G., Marcoux, C., Hentz, S., Andreucci, P. & Roukes, M. (2009). Piezoelectric nanoelectromechanical resonators based on aluminum nitride thin films. *Applied Physics Letters*, 95(10), 103111.

Khisaeva, Z. & Ostoja-Starzewski, M. (2006). Thermoelastic damping in nanomechanical resonators with finite wave speeds. *Journal of Thermal stresses*, 29(3), 201–216.

Kim, B., Melamud, R., Candler, R., Hopcroft, M., Jha, C., Chandorkar, S. & Kenny, T. (2010). Encapsulated MEMS resonators—A technology path for MEMS into frequency control applications. *2010 IEEE International Frequency Control Symposium*, pp. 1–4.

Kim, B., Candler, R. N., Hopcroft, M. A., Agarwal, M., Park, W.-T. & Kenny, T. W. (2007). Frequency stability of wafer-scale film encapsulated silicon based MEMS resonators. *Sensors and Actuators A: Physical*, 136(1), 125–131.

Kovacs, G. T., Maluf, N. I. & Petersen, K. E. (1998). Bulk micromachining of silicon. *Proceedings of the IEEE*, 86(8), 1536–1551.

Kumar, H. & Mukhopadhyay, S. (2020). Thermoelastic damping analysis for size-dependent microplate resonators utilizing the modified couple stress theory and the three-phase-lag heat conduction model. *International Journal of Heat and Mass Transfer*, 148, 118997.

Kumar Mishra, M., Mishra, P., Dubey, V., Khan, I. & Sachdev, T. (2021). A Review for Luminescence Property of Materials, Its Detection and Probabilities for Embedding of Luminescence with MEMS Technology. *Advanced Materials Letters*, 12(5), 1–9.

Kunal, K. & Aluru, N. (2011). Akhiezer damping in nanostructures. *Physical Review B*, 84(24), 245450.

Lam, C. (2016). A review of the timing and filtering technologies in smartphones. *2016 IEEE International Frequency Control Symposium (IFCS)*, pp. 1–6.

Lavasani, H. M., Pan, W., Harrington, B. P., Abdolvand, R. & Ayazi, F. (2012). Electronic temperature compensation of lateral bulk acoustic resonator reference oscillators using enhanced series tuning technique. *IEEE Journal of Solid-State Circuits*, 47(6), 1381–1393.

Lee, H., Partridge, A. & Assaderaghi, F. (2012). Low jitter and temperature stable MEMS oscillators. *2012 IEEE International Frequency Control Symposium Proceedings*, pp. 1–5.

Lee, H. K., Melamud, R., Kim, B., Hopcroft, M. A., Salvia, J. C. & Kenny, T. W. (2011). Electrostatic tuning to achieve higher stability microelectromechanical composite resonators. *Journal of microelectromechanical systems*, 20(6), 1355–1365.

Li, C., Wen, H., Wisher, S., Norouzpour-Shirazi, A., Lei, J.-Y., Chen, H. & Ayazi, F. (2019). An FPGA-based interface system for high-frequency bulk-acoustic-wave microgyroscopes with in-run automatic mode-matching. *IEEE Transactions on Instrumentation and Measurement*, 69(4), 1783–1793.

Lim, A. V., Karacolak, T., Jiang, J.-Y., Huang, C.-F. & Zhao, F. (2015). Electrostatically-actuated 4H-SiC in-plane and out-of-plane high frequency MEMS resonator. *IEEE Microwave and wireless components letters*, 26(1), 28–30.

Lin, T.-H. (1996). Flexure-beam micromirror devices and potential expansion for smart micromachining. *Smart Structures and Materials 1996: Smart Electronics and MEMS*, 2722, 20–29.

Linder, C., Paratte, L., Grétillat, M.-A., Jaecklin, V. & De Rooij, N. (1992). Surface micromachining. *Journal of Micromechanics and Microengineering*, 2(3), 122.

Lipiäinen, L., Jaakkola, A., Kokkonen, K. & Kaivola, M. (2012). Nonlinear excitation of a rotational mode in a piezoelectrically excited square-extensional mode resonator. *Applied Physics Letters*, 100(15), 153508.

Liu, C.-H., Chang, H.-D., Li, K.-H., Lin, C.-H., Hsu, C.-J., Lin, T.-Y., Chou, H.-H., Huang, H.-C. & Liao, H.-Y. (2013). Adaptable and integrated packaging platform for MEMS-based combo sensors utilizing innovative wafer-level packaging technologies. *2013 IEEE 63rd Electronic Components and Technology Conference*, pp. 1675–1681.

Liu, J., Workie, T. B., Wu, T., Wu, Z., Gong, K., Bao, J. & Hashimoto, K.-y. (2020). Q-factor enhancement of thin-film piezoelectric-on-silicon mems resonator by phononic crystal-reflector composite structure. *Micromachines*, 11(12), 1130.

Loebl, H., Klee, M., Metzmacher, C., Brand, W., Milsom, R. & Lok, P. (2003). Piezoelectric thin AlN films for bulk acoustic wave (BAW) resonators. *Materials Chemistry and Physics*, 79(2-3), 143–146.

Loops, M. P.-L. (1996). *Monolithic phase-locked loops and clock recovery circuits*. IEEE press.

Lutz, M., McDonald, J., Gupta, P., Partridge, A., Dimpel, C. & Petersen, K. (2007a). New MEMS timing references for automotive applications. *Advanced Microsystems for Automotive Applications*, pp. 279–289.

Lutz, M., Partridge, A., Gupta, P., Buchan, N., Klaassen, E., McDonald, J. & Petersen, K. (2007b). MEMS oscillators for high volume commercial applications. *TRANSDUCERS 2007-2007 International Solid-State Sensors, Actuators and Microsystems Conference*, pp. 49–52.

Matsumoto, K., Kadota, M. & Tanaka, S. (2020). High frequency thickness expansion mode bulk acoustic wave resonator using LN single crystal thin plate. *Japanese Journal of Applied Physics*, 59(3), 036506.

Mattila, T., Kiihamäki, J., Lamminmäki, T., Jaakkola, O., Rantakari, P., Oja, A., Seppä, H., Kattelus, H. & Tittonen, I. (2002). A 12 MHz micromechanical bulk acoustic mode oscillator. *Sensors and Actuators A: Physical*, 101(1-2), 1–9.

Mccann, D. F., Mcgann, J. M., Parks, J. M., Frankel, D. J., Da Cunha, M. P. & Vetelino, J. F. (2009). A lateral-field-excited LiTaO 3 high-frequency bulk acoustic wave sensor. *IEEE transactions on ultrasonics, ferroelectrics, and frequency control*, 56(4), 779–787.

Mei, J. & Li, L. (2013). Frequency self-tuning of carbon nanotube resonator with application in mass sensors. *Sensors and Actuators B: Chemical*, 188, 661–668.

Melamud, R., Hagelin, P., Arft, C., Grosjean, C., Arumugam, N., Gupta, P., Hill, G., Lutz, M., Partridge, A. & Assaderaghi, F. (2012). MEMS enables oscillators with sub-ppm frequency stability and sub-ps jitter. *Proc. Solid-State Sens., Actuators, Microsyst. Workshop*, pp. 66–69.

Melamud, R., Hopcroft, M., Jha, C., Kim, B., Chandorkar, S., Candler, R. & Kenny, T. W. (2005). Effects of stress on the temperature coefficient of frequency in double clamped resonators. *The 13th International Conference on Solid-State Sensors, Actuators and Microsystems, 2005. Digest of Technical Papers. TRANSDUCERS'05.*, 1, 392–395.

Mishra, M. K., Dubey, V., Mishra, P. & Khan, I. (2019). MEMS technology: A review. *J. Eng. Res. Rep*, 4(1), 1–24.

Molarius, J., Kaitila, J., Pensala, T. & Ylilammi, M. (2003). Piezoelectric ZnO films by rf sputtering. *Journal of Materials Science: Materials in Electronics*, 14(5), 431–435.

Nabavi, S. & Bhadra, S. (2021). Efficient and Easy to Fabricate Silicon-Based Planar Micro-Coils for Wireless Power Transfer Applications. *IEEE Sensors Journal*, 22(3), 1980–1989.

Nabavi, S., Aljaroudi, A. & Zhang, L. (2018). T-shaped piezoelectric vibratory MEMS harvester with integration of highly efficient power management system. *Journal of Physics: Conference Series*, 1052(1), 012102.

Nabavi, S., Ménard, M. & Nabki, F. (2022). A SOI out-of-plane electrostatic MEMS actuator based on in-plane motion. *Journal of Microelectromechanical Systems*, 31(5), 820–829.

Ng, E., Yang, Y., Hong, V., Ahn, C., Heinz, D., Flader, I., Chen, Y., Everhart, C., Kim, B., Melamud, R. et al. (2015). The long path from MEMS resonators to timing products. *2015 28th IEEE International Conference on Micro Electro Mechanical Systems (MEMS)*, pp. 1–2.

Nguyen, C. T.-C. (2007). MEMS technology for timing and frequency control. *IEEE transactions on ultrasonics, ferroelectrics, and frequency control*, 54(2), 251–270.

Nguyen, C.-C. (1999). Frequency-selective MEMS for miniaturized low-power communication devices. *IEEE Transactions on Microwave Theory and Techniques*, 47(8), 1486–1503.

Pachkawade, V. (2020). Ultra-precise MEMS based bio-sensors. *Biosensor-Current and Novel Strategies for Biosensing*.

Pal, P. & Sato, K. (2017). *Silicon wet bulk micromachining for MEMS*. Jenny Stanford Publishing.

Pal, P., Swarnalatha, V., Rao, A. V. N., Pandey, A. K., Tanaka, H. & Sato, K. (2021). High speed silicon wet anisotropic etching for applications in bulk micromachining: a review. *Micro and Nano Systems Letters*, 9, 1–59.

Park, Y.-H. & Park, K. (2004). High-fidelity modeling of MEMS resonators. part ii. coupled beam-substrate dynamics and validation. *Journal of Microelectromechanical Systems*, 13(2), 248–257.

Partridge, A., Lee, H.-C., Hagelin, P. & Menon, V. (2013). We know that MEMS is replacing quartz. But why? And why now? *2013 Joint European Frequency and Time Forum & International Frequency Control Symposium (EFTF/IFC)*, pp. 411–416.

Pavithra, M., Sathya, S. & Muruganand, S. (2015). Design and modeling of nonlinear coupled MEMS resonator using electrostatic actuation for L-band mobile satellite communication. *Int. J. ChemTech Res*, 7(2), 678–684.

Piazza, G., Felmetsger, V., Muralt, P., Olsson III, R. H. & Ruby, R. (2012). Piezoelectric aluminum nitride thin films for microelectromechanical systems. *MRS bulletin*, 37(11), 1051–1061.

Pillai, G. & Li, S.-S. (2020). Piezoelectric MEMS resonators: A review. *IEEE Sensors Journal*, 21(11), 12589–12605.

Platz, D. & Schmid, U. (2019). Vibrational modes in MEMS resonators. *Journal of Micromechanics and Microengineering*, 29(12), 123001.

Puder, J., Bedair, S., Pulskamp, J., Rudy, R., Polcawich, R. & Bhave, S. (2015). Higher dimensional flexure mode for enhanced effective electromechanical coupling in PZT-on-silicon MEMS resonators. *2015 Transducers-2015 18th International Conference on Solid-State Sensors, Actuators and Microsystems (TRANSDUCERS)*, pp. 2017–2020.

Qaradaghi, V., Mahdavi, M., Kumar, V. & Pourkamali, S. (2016). Frequency output MEMS resonator on membrane pressure sensors. *2016 IEEE SENSORS*, pp. 1–3.

Rangelow, I. W. (2001). Dry etching-based silicon micro-machining for MEMS. *Vacuum*, 62(2-3), 279–291.

Reicher, D. W., Christian, R., Davidson, P. & Peplinski, S. Z. (2009). Use of multiple DC magnetron deposition sources for uniform coating of large areas. *Thin Film Solar Technology*, 7409, 31–41.

Rodriguez, J., Gerrard, D. D., Glaze, G. M., Chandorkar, S., Comenecia, L., Chen, Y., Flader, I. B. & Kenny, T. W. (2017). Direct measurements of anchor damping in MEMS resonators. *2017 IEEE SENSORS*, pp. 1–3.

Rodriguez, J., Chandorkar, S. A., Glaze, G. M., Gerrard, D. D., Chen, Y., Heinz, D. B., Flader, I. B. & Kenny, T. W. (2018). Direct detection of anchor damping in MEMS tuning fork resonators. *Journal of Microelectromechanical Systems*, 27(5), 800–809.

Rodriguez, J., Chandorkar, S. A., Watson, C. A., Glaze, G. M., Ahn, C. H., Ng, E. J., Yang, Y. & Kenny, T. W. (2019). Direct Detection of Akhiezer Damping in a Silicon MEMS Resonator. *Scientific Reports*, 9(1), 2244. doi: 10.1038/s41598-019-38847-6.

Rudy, R. Q., Pulskamp, J. S., Bedair, S. S., Puder, J. M. & Polcawich, R. G. (2016). Piezoelectric disk flexure resonator with 1 dB loss. *2016 IEEE international frequency control symposium (IFCS)*, pp. 1–4.

Sastry, D. (2009). Radio Frequency Microelectromechanical Systems in Defence and Aerospace. *Defence Science Journal*, 59(6).

Schaal, C., M'Closkey, R. & Mal, A. (2018). Semi-analytical modeling of anchor loss in plate-mounted resonators. *Ultrasonics*, 82, 304–312.

Schiwietz, D., Weig, E. M. & Degenfeld-Schonburg, P. (2022). Thermoelastic Damping in MEMS Gyroscopes at High Frequencies. *arXiv preprint arXiv:2208.02591*.

Segovia-Fernandez, J. & Piazza, G. (2016). Analytical and numerical methods to model anchor losses in 65-MHz AlN contour mode resonators. *Journal of Microelectromechanical Systems*, 25(3), 459–468.

Segovia-Fernandez, J. & Piazza, G. (2017). Thermoelastic damping in the electrodes determines $ Q $ of AlN contour mode resonators. *Journal of Microelectromechanical Systems*, 26(3), 550–558.

Serrano, D. E., Tabrizian, R. & Ayazi, F. (2011). Tunable piezoelectric MEMS resonators for real-time clock. *2011 Joint Conference of the IEEE International Frequency Control and the European Frequency and Time Forum (FCS) Proceedings*, pp. 1–4.

Shahmohammadi, M., Modarres-Zadeh, M. J. & Abdolvand, R. (2010). Low jitter thin-film piezoelectric-on-substrate oscillators. *2010 IEEE International Frequency Control Symposium*, pp. 613–617.

Shao, L., Palaniapan, M., Khine, L. & Tan, W. (2008). Nonlinear behavior of Lamé-mode SOI bulk resonator. *2008 IEEE International Frequency Control Symposium*, pp. 646–650.

Siddiqi, M. W. U., Fedeli, P., Tu, C., Frangi, A. & Lee, J. E. (2019). Numerical analysis of anchor loss and thermoelastic damping in piezoelectric AlN-on-Si Lamb wave resonators. *Journal of Micromechanics and Microengineering*, 29(10), 105013.

Sorenson, L. & Ayazi, F. (2014). Effect of structural anisotropy on anchor loss mismatch and predicted case drift in future micro-hemispherical resonator gyros. *Proceedings of IEEE/ION PLANS 2014*, pp. 493–498.

Sridaran, S. & Bhave, S. A. (2011). Electrostatic actuation of silicon optomechanical resonators. *Optics express*, 19(10), 9020–9026.

Sutagundar, M., Sheeparamatti, B. & Jangamshetti, D. (2014). Research issues in MEMS resonators. *Research Inventy: International Journal of Engineering & Science 2014*, 4(8).

Svilicic, B., Mastropaolo, E., Flynn, B. & Cheung, R. (2012). Electrothermally actuated and piezoelectrically sensed silicon carbide tunable MEMS resonator. *IEEE electron device letters*, 33(2), 278–280.

Tai, Y. & Chen, N. (2019). Thermoelastic damping in the out-of-plane vibration of a microring resonator with rectangular cross-section. *International Journal of Mechanical Sciences*, 151, 684–691.

Takeshita, T., Nguyen, T.-V., Daniel, Z., Takei, Y. & Kobayashi, T. (2022). Mechanical characteristics of laminated film vibrator using an ultra-thin MEMS actuator. *Journal of Micromechanics and Microengineering*, 32(10), 105001.

Teixeira, F. & Chew, W. (2000). Complex space approach to perfectly matched layers: a review and some new developments. *International Journal of Numerical Modelling: Electronic Networks, Devices and Fields*, 13(5), 441–455.

Thakar, V. A., Wu, Z., Peczalski, A. & Rais-Zadeh, M. (2013). Piezoelectrically transduced temperature-compensated flexural-mode silicon resonators. *Journal of microelectromechanical systems*, 22(3), 815–823.

Tilmans, H. A., Elwenspoek, M. & Fluitman, J. H. (1992). Micro resonant force gauges. *Sensors and Actuators A: Physical*, 30(1-2), 35–53.

Tiwari, S. & Candler, R. N. (2019). Using flexural MEMS to study and exploit nonlinearities: A review. *Journal of Micromechanics and Microengineering*, 29(8), 083002.

Tocchio, A., Caspani, A. & Langfelder, G. (2011). Mechanical and electronic amplitude-limiting techniques in a MEMS resonant accelerometer. *IEEE Sensors journal*, 12(6), 1719–1725.

Toshiyoshi, H., Ju, S., Honma, H., Ji, C.-H. & Fujita, H. (2019). MEMS vibrational energy harvesters. *Science and technology of advanced materials*, 20(1), 124–143.

Trolier-McKinstry, S. & Muralt, P. (2004). Thin film piezoelectrics for MEMS. *Journal of Electroceramics*, 12(1), 7–17.

Turkel, E. & Yefet, A. (1998). Absorbing PML boundary layers for wave-like equations. *Applied Numerical Mathematics*, 27(4), 533–557.

Varanis, M., Silva, A., Mereles, A. & Pederiva, R. (2018). MEMS accelerometers for mechanical vibrations analysis: A comprehensive review with applications. *Journal of the Brazilian Society of Mechanical Sciences and Engineering*, 40(11), 1–18.

Verbridge, S. S., Shapiro, D. F., Craighead, H. G. & Parpia, J. M. (2007). Macroscopic tuning of nanomechanics: substrate bending for reversible control of frequency and quality factor of nanostring resonators. *Nano Letters*, 7(6), 1728–1735.

Wang, E., Carcione, J. M., Ba, J., Alajmi, M. & Qadrouh, A. N. (2019). Nearly perfectly matched layer absorber for viscoelastic wave equations. *Geophysics*, 84(5), T335-T345. doi: 10.1190/geo2018-0732.1.

Wang, L., Wang, C., Wang, Y., Quan, A., Keshavarz, M., Madeira, B. P., Zhang, H., Wang, C. & Kraft, M. (2022). A Review on Coupled Bulk Acoustic Wave MEMS Resonators. *Sensors*, 22(10), 3857.

Wang, X., Huan, R., Pu, D. & Wei, X. (2018). Effect of nonlinearity and axial force on frequency drift of a T-shaped tuning fork micro-resonator. *Journal of Micromechanics and Microengineering*, 28(12), 125012.

Weinstein, D., Bhave, S. A., Tada, M., Mitarai, S., Morita, S. & Ikeda, K. (2007). Mechanical coupling of 2D resonator arrays for MEMS filter applications. *2007 IEEE International Frequency Control Symposium Joint with the 21st European Frequency and Time Forum*, pp. 1362–1365.

Weng, C.-H., Pillai, G. & Li, S.-S. (2020). A thin-film piezoelectric-on-silicon MEMS oscillator for mass sensing applications. *IEEE Sensors Journal*, 20(13), 7001–7009.

Workie, T. B., Wu, T., Bao, J.-F. & Hashimoto, K.-y. (2021). Design for high-quality factor of piezoelectric-on-silicon MEMS resonators using resonant plate shape and phononic crystals. *Japanese Journal of Applied Physics*, 60(SD), SDDA03.

Wu, G., Xu, J., Ng, E. J. & Chen, W. (2020). MEMS resonators for frequency reference and timing applications. *Journal of Microelectromechanical Systems*, 29(5), 1137–1166.

Wu, X., Bao, F., Zhou, X., Wu, Q., Liu, J. & Bao, J. (2019). Spider Web-Shaped Phononic Crystals for Quality Factor Improvement of Piezoelectric-on-Silicon MEMS resonators. *2019 IEEE International Ultrasonics Symposium (IUS)*, pp. 1724–1726. doi: 10.1109/ULTSYM.2019.8926212.

Xu, J., Chai, K. T.-C., Wu, G., Han, B., Wai, E. L.-C., Li, W., Yeo, J., Nijhof, E. & Gu, Y. (2018). Low-cost, tiny-sized MEMS hydrophone sensor for water pipeline leak detection. *IEEE Transactions on Industrial Electronics*, 66(8), 6374–6382.

Yang, R., Ladhane, K., Wang, Z., Lee, J., Young, D. J. & Feng, P. X.-L. (2014). Smart-cut 6H-silicon carbide (SiC) microdisk torsional resonators with sensitive photon radiation detection. *2014 IEEE 27th International Conference on Micro Electro Mechanical Systems (MEMS)*, pp. 793–796.

Yang, R., Zorman, C. A. & Feng, P. X.-L. (2015). High frequency torsional-mode nanomechanical resonators enabled by very thin nanocrystalline diamond diaphragms. *Diamond and Related Materials*, 54, 19–25.

Yasumura, K. Y., Stowe, T. D., Chow, E. M., Pfafman, T., Kenny, T. W., Stipe, B. C. & Rugar, D. (2000). Quality factors in micron-and submicron-thick cantilevers. *Journal of microelectromechanical systems*, 9(1), 117–125.

Yi, Y. (2008). Geometric effects on thermoelastic damping in MEMS resonators. *Journal of Sound and Vibration*, 309(3-5), 588–599.

Zener, C. (1937). Internal friction in solids. I. Theory of internal friction in reeds. *Physical review*, 52(3), 230.

Zener, C. (1938). Internal friction in solids II. General theory of thermoelastic internal friction. *Physical review*, 53(1), 90.

Zhang, G., Zhao, L., Xu, L., Jiang, Z., Zhao, Y., Wang, X. & Liu, Z. (2013). Active frequency tuning for magnetically actuated and piezoresistively sensed MEMS resonators. *IEEE electron device letters*, 34(7), 921–923.

Zhang, H., Zhang, C., Chen, J. & Li, A. (2022). A Review of Symmetric Silicon MEMS Gyroscope Mode-Matching Technologies. *Micromachines*, 13(8), 1255.

Zhang, H., Kim, T., Choi, G. & Cho, H. H. (2016). Thermoelastic damping in micro-and nanomechanical beam resonators considering size effects. *International Journal of Heat and Mass Transfer*, 103, 783–790.

Zhang, M., Luiz, G., Shah, S., Wiederhecker, G. & Lipson, M. (2014). Eliminating anchor loss in optomechanical resonators using elastic wave interference. *Applied Physics Letters*, 105(5), 051904.

Zhang, W.-M., Hu, K.-M., Peng, Z.-K. & Meng, G. (2015). Tunable micro-and nanomechanical resonators. *Sensors*, 15(10), 26478–26566.

Zhang, Z., Wu, Y., Sang, L., Wu, H., Huang, J., Wang, L., Takahashi, Y., Li, R., Koizumi, S. & Toda, M. (2020). Coupling of magneto-strictive FeGa film with single-crystal diamond MEMS resonator for high-reliability magnetic sensing at high temperatures. *Materials Research Letters*, 8(5), 180–186.

Zhao, C., Montaseri, M. H., Wood, G. S., Pu, S. H., Seshia, A. A. & Kraft, M. (2016). A review on coupled MEMS resonators for sensing applications utilizing mode localization. *Sensors and Actuators A: Physical*, 249, 93–111.

Zhao, C., Pandit, M., Sobreviela, G., Steinmann, P., Mustafazade, A., Zou, X. & Seshia, A. (2019). A resonant MEMS accelerometer with 56ng bias stability and 98ng/Hz 1/2 noise floor. *Journal of Microelectromechanical Systems*, 28(3), 324–326.

Zhu, H., Shan, G., Shek, C. & Lee, J.-Y. (2012). Shear dependent nonlinear vibration in a high quality factor single crystal silicon micromechanical resonator. *Applied Physics Letters*, 101(3), 034102.

Zou, H., Wang, J. & Li, X. (2017). High-performance low-range differential pressure sensors formed with a thin-film under bulk micromachining technology. *Journal of Microelectromechanical Systems*, 26(4), 879–885.

Zuo, C., Rinaldi, M. & Piazza, G. (2009). Power handling and related frequency scaling advantages in piezoelectric AlN contour-mode MEMS resonators. *2009 IEEE International Ultrasonics Symposium*, pp. 1187–1190.